Geosphere

# Deformation and structure in the Chugach metamorphic complex, southern Alaska: Crustal architecture of a transpressional system from a down plunge section

Mitchell R. Scharman, Terry L. Pavlis, Erik M. Day and Leland J. O'Driscoll

*Geosphere* 2011;7;992-1012
doi: 10.1130/GES00646.1



**Notes**



# Deformation and structure in the Chugach metamorphic complex, southern Alaska: Crustal architecture of a transpressional system from a down plunge section

**Mitchell R. Scharman[1], Terry, L. Pavlis[1], Erik M. Day[1], and Leland J. O'Driscoll[2]**
[1]*Department of Geological Science, University of Texas at El Paso, El Paso, Texas 79968, USA*
[2]*Department of Geological Sciences, University of Oregon, Eugene, Oregon 97403, USA*

## ABSTRACT

**Multiple Paleogene dextral shear zones are identified in the Chugach metamorphic complex (CMC) in southern Alaska providing an unusual down-plunge view of the deformation associated with transpressional strike-slip systems at mid- to lower-crustal levels. Along the northern flank of the CMC, the brittle Stuart Creek fault is structurally continuous with the ductile Harry's Gulch shear zone. Field relationships suggest the brittle fault transfers slip structurally downward into a localized, ~2-km-wide shear zone deformed under greenschist-facies conditions. At amphibolite-facies, under mid-crustal conditions, deformation is localized in anastomosing shear zones ranging from 10s of m to 2–3 km in width that are cryptic as they pass downward into lower-crustal migmatitic gneiss. Strike-slip–related deformation in these migmatitic gneisses is more dispersed, suggesting more distributed flow. Absence of a symmetric cleavage fan associated with the steep ductile shear zones and variations in finite strain indicate that an attachment zone model (e.g., Teyssier and Cruz, 2004) is not applicable to the deep crustal structure of the CMC strike-slip system. We discuss two as yet indistinguishable hypotheses to account for the deep crustal structure of the CMC strike-slip system: (1) a narrow detachment zone model where detachment occurs at the metamorphic transition from schist to gneiss, and (2) a differential folding model where crustal-penetrating shear zones are masked by variations in folding mechanisms at different crustal levels.**

## INTRODUCTION

The structure of strike-slip fault systems at the mid- and lower-crust depths remains a first-order, unresolved question in tectonics. Early models of strike-slip systems assumed that discrete faults in the upper crust simply transitioned downward into broad shear zones below the brittle-ductile transition (e.g., Scholz, 1990, p. 129). However, as evidence accumulated on the widespread occurrence of transrotational zones along many continental strike-slip systems (Dewey et al., 1998) and dispersed zones of deformation in all continental strike-slip systems ranging from transtension to transpressional settings (e.g., Fitch, 1972; Karig, 1980; Serpa and Pavlis, 1996; Dewey, 2002) it has become clear that the initial view of fault behavior in strike-slip systems oversimplifies the problem. In particular, distribution of strike-slip over a broad band of continental crust requires either distinct microplate lozenges separated by steep lithospheric shear zones, or some form of detachment must occur within the lithosphere if the strike-slip shear zones do not penetrate to the asthenosphere (e.g., Thatcher, 1995). Recent numerical modeling suggests that strike-slip systems in the mid- and lower crust (10–30 km, depending on geotherm) form either a horizontal attachment zone or a detachment zone that accommodates flow between localized zones of horizontal shearing above and a widespread, homogenous zone of wrench shearing below (e.g., Teyssier and Cruz, 2004).

The Chugach terrane, located in southern Alaska, is a late Mesozoic to Eocene accretionary prism that has experienced northward transport along several strike-slip fault systems during oblique subduction in association with a ridge-subduction event (Fig. 1; Pavlis and Sisson, 1995). The eastern part of the Chugach terrane is the Chugach metamorphic complex (CMC), a high-temperature/low-pressure metamorphic belt superimposed upon the accretionary prism assemblages of the Chugach terrane during the Eocene ridge subduction event (e.g., Sisson et al., 1989; Sisson and Pavlis, 1993; Hauessler et al., 1995; Bradley et al., 2003). The western termination of the CMC represents a down-plunge view of the crustal section in this region, ranging from prehenite-pumpellyite and low greenschist metamorphic grades in the west, to upper amphibolite metamorphic grade within the core of the complex (e.g., Sisson et al., 1989; Dusel-Bacon et al., 1994). This oblique crustal section exhumes a strike-slip system that developed within the accretionary complex during the ridge subduction event (e.g., Pavlis and Sisson, 2003).

This study focuses on results from field studies examining the crustal architecture of this down-plunge view of a strike-slip system, and tested the attachment zone hypothesis of Teyssier and Cruz (2004). It became apparent after fieldwork that this model could not explain the overall structure identified from the field observations. In this paper, we emphasize the general structural architecture recognized in the CMC strike-slip system, particularly the transition from brittle to ductile deformation in a strike-slip shear zone, and the occurrence of an asymmetric cleavage pattern developed through dextral transpression. We compare these observations to the predictions of the attachment zone model, and conclude that this is not a viable explanation for the structure of the CMC. Our observations lead us to evaluate two alternative hypotheses for the deep crustal structure of the strike-slip system: (1) a regional detachment

*Geosphere*; August 2011; v. 7; no. 4; p. 992–1012; doi: 10.1130/GES00646.1; 7 figures; 1 table; 5 plates; 1 supplemental file.

system at the transition from schist to gneiss, or (2) differential folding producing variable folding mechanisms that mask crustal-penetrating shear zones at different levels. We conclude that these hypotheses are not yet easily distinguished and further work is needed on structural details within the gneissic core of the complex.

## TECTONIC AND GEOLOGIC BACKGROUND

The Chugach terrane in south-central Alaska is an accretionary complex exposed along the Border Ranges fault that has a protracted history of tectonic transport, deformation, metamorphism, and magmatism during Mesozoic subduction along the northern Cordilleran margin. The complex consists of two distinct accretionary assemblages (Plafker et al., 1994): (1) an older, Jurassic to middle Cretaceous mélange assemblage that is exposed along the crystalline backstop to the accretionary complex (Amato and Pavlis, 2010); and (2) a younger, late Cretaceous assemblage comprised of interbedded graywacke and argillite that are generally interpreted as trench-fill turbidites (Plafker et al., 1989). In most of southern Alaska, the Chugach terrane is a low-grade metamorphic complex comprised of slates and phyllites at prehnite-pumpellyite to lower greenschist facies (Dusel-Bacon, 1994). In the eastern Chugach Mountains, however, metamorphic grade rises eastward from the biotite zone near Valdez to upper amphibolite facies, high-temperature/low-pressure metamorphic assemblages east of the Copper River (Figs. 1 and 2). These high-grade rocks and associated plutons are referred to regionally as the Chugach metamorphic complex (Hudson and Plafker, 1982). The high-temperature/low-pressure metamorphism is indicated by andalusite-sillimanite assemblages without kyanite throughout the amphibolite facies schists of the Chugach metamorphic complex (CMC), abundance of cordierite in amphibolite facies schists and gneisses, and local thermobarometry studies (Sisson et al., 1989, 2003; Pavlis and Sisson, 1995, 2003). Recent studies by Gasser et al. (2011) have suggested that peak pressures may have been much higher in the gneiss core of the complex, suggesting potential complications to the general high-temperature/low-pressure metamorphism, but further work is needed to clarify this problem.

Metamorphism of the CMC is only part of the broader, regional manifestations of an anomalous emplacement of the Sanak-Baranof plutonic belt (Marshak and Karig, 1977; Hudson, 1979; Hudson et al., 1979; Badley et al., 2003) that swept through the Alaskan forearc from latest Cretaceous to middle Eocene time. CMC metamorphism and Sanak-Baranof plutonism are widely recognized as the product of ridge subduction during latest Cretaceous and Paleogene time (e.g., Sisson et al., 1989; Sisson and Pavlis, 1993; Bradley et al., 2003).

Previous analyses of deformational fabrics within the CMC have identified various crustal flow regimes within the complex (Sisson and Pavlis, 1993; Pavlis and Sisson, 1995, 2003). Fabrics in the CMC identified by previous researchers and by our own observations are summarized in Table 1. An initial deformational phase ($D_1$) produces a layer-parallel, pressure-solution foliation ($S_1$). Two dominant deformational phases ($D_2$ and $D_3$) have been identified and are described as either an overprinting sequence related to changing plate motions (e.g., Pavlis and Sisson, 1995) or as broadly coeval fabrics that are diachronous (Pavlis and Sisson, 2003). Within the lower-grade schist assemblage of the CMC, $D_2$ produces foliations that are generally shallowly dipping ($S_2$) with foliation axial planar to recumbent to gently inclined $D_2$ folds ($F_{2AP}$). $S_2$ is a mica foliation defined primarily by biotite, but also muscovite and chlorite, and is the result of progressive folding of the earlier $S_1$ foliation. The $D_2$ fabrics are in turn overprinted by $D_3$ structures that produce subvertical foliations ($S_3$) in discrete localized zones but vary with structural level (Sisson and Pavlis, 1993). $S_3$ is axial planar to $D_3$ folds and is primarily a crenulation cleavage. A regional $D_2$ downward-convergent foliation fan was proposed for the

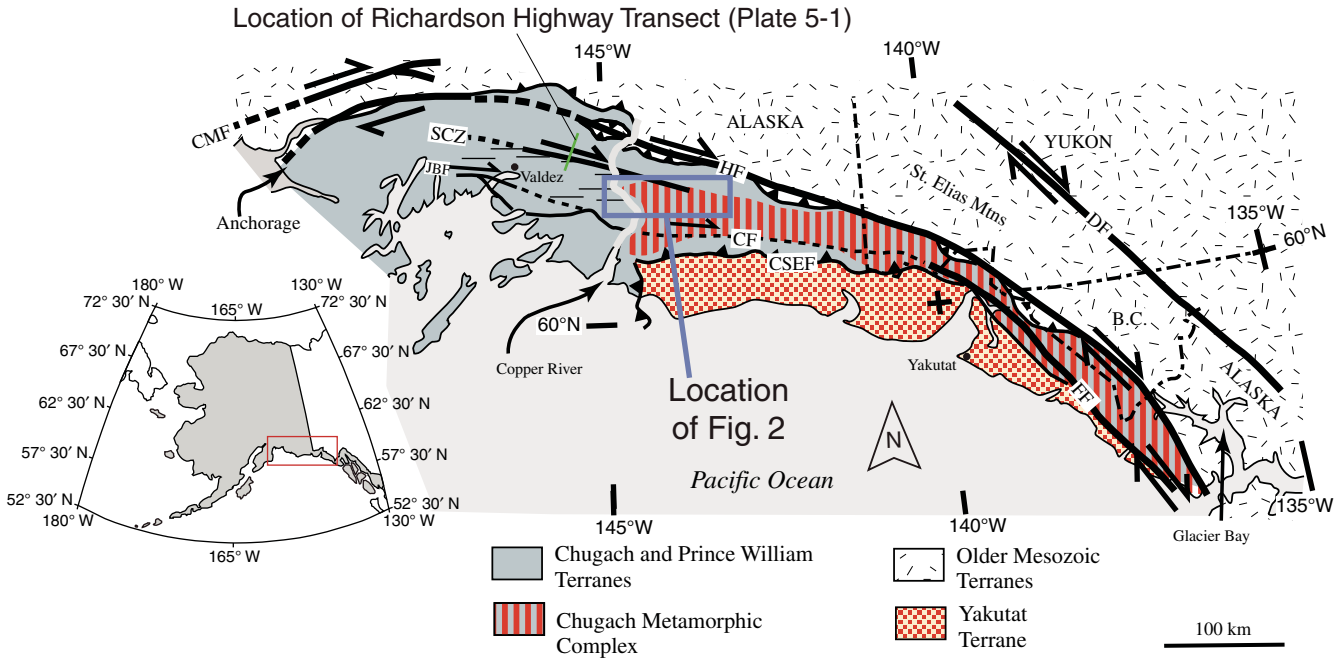


**Figure 1. Generalized tectonic map of the Chugach metamorphic complex, southern Alaska. FF—Fairweather fault, CSEF—Chugach-St. Elias fault, CF—Contact fault, HF—Hanagita fault, SCZ—Stuart Creek zone, JBF—Jack Bay fault, CMF—Castle Mountain fault, DF—Denali fault. Figure is modified from Pavlis and Sisson (2003) which was derived from Hudson and Plafker (1982); Dusel-Bacon et al. (1994); and mapping of Sisson, Pavlis, Cooper, Roeske, Marty, and Poole.**

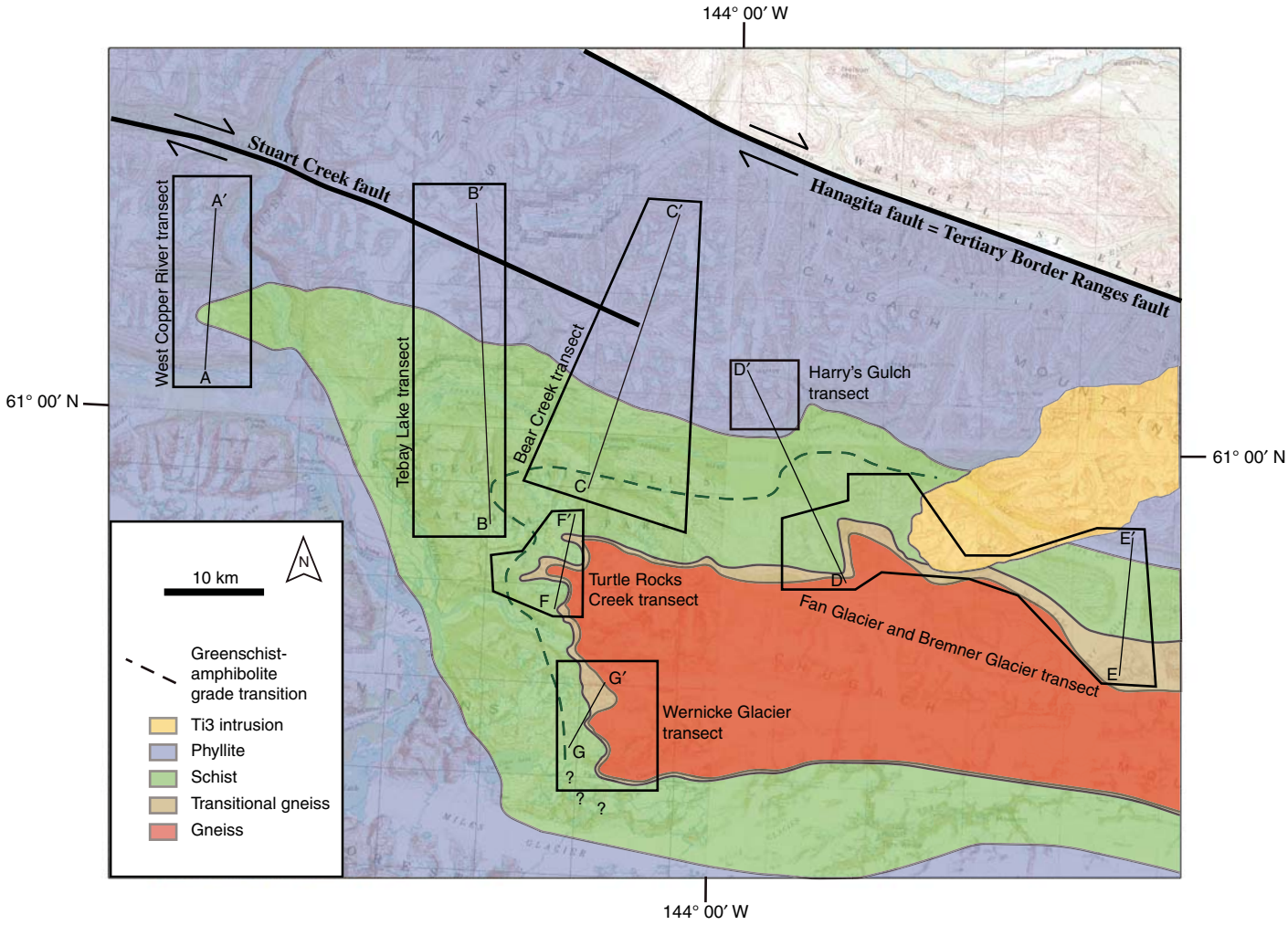


**Figure 2. Regional map of the Chugach metamorphic complex, with locations of field areas described in this paper. Location of the Richardson Highway transect shown in Figure 1. Geologic contacts and isograds from geologic mapping presented in this paper, and regional mapping by Hudson and Plafker (1982). Mapping modified from Richter et al. (2005).**

structure on the northwestern side of the CMC in the lower-grade schist (O'Driscoll, 2006; Day, 2007). However, in the gneissic core of the CMC, $D_3$ folds deform $S_2$ foliations, with an associated continuous, axial planar $S_3$ foliation (Sisson and Pavlis, 1993). This difference in orientations of foliations between the enveloping schist and the gneissic core suggest a change in mid-crustal flow across the structural/metamorphic transition from schist to gneiss (Pavlis and Sisson, 2003). Extensional lineations are found on $D_2$ foliation planes in the CMC, but the orientation of the lineations varies within the CMC. Extensional lineations are found to trend approximately east-west and plunge subhorizontally in locations on the northern side of the CMC, whereas extensional lineations are found to plunge down-dip on the southern side of the CMC (Pavlis and Sis-

TABLE 1. CMC FABRIC DESCRIPTIONS

| Phase | Fabric | Description |
|---|---|---|
| $D_1$ | $S_0/S_1$ | Layer-parallel pressure-solution foliation, variable dip due to folding by younger deformation |
| $D_2$ | $F_{2AP}$ | Axial planes of folds formed during $D_2$ |
| $D_2$ | $L_{F2}$ | $F_2$ axis orientation, east-west trend, subhorizontal plunge |
| $D_2$ | $S_2$ | Predominant mica foliation throughout the CMC, generally, shallow to moderate dip, axial planar to $F_2$ |
| $D_2$ | $L_{ext}$ | Extensional lineation, east-west trend, subhorizontal plunge, located on $S_2$ foliation planes |
| $D_2$ | $S_{gw}$ | Finite strain foliation observed in layers of metagraywacke, variable dip; commonly equivalent to $S_2$ but shows different orientations where $D_2$-$D_3$ overprints are complex |
| $D_2$ | $L_{gw}$ | Extensional and intersection lineation, subhorizontal plunge, located on $S_{gw}$ foliation planes |
| $D_3$ | $F_{3AP}$ | Subvertical axial planes formed during $D_3$ by deforming older fabrics |
| $D_3$ | $L_{F3}$ | $F_3$ axis orientation, east-west trend, subhorizontal plunge |
| $D_3$ | $S_3$ | Subvertical, crenulation cleavage, axial planar to $F_3$ |

*Note*: Fabric descriptions from field observations and Sisson and Pavlis (1993); Pavlis and Sisson (1995, 2003).

son, 2003; Gasser, 2010). The variety of orientations for extensional lineations also indicates variations in strain and crustal flow across the CMC (Pavlis and Sisson, 2003).

It has long been known that the deformation periods of $D_2$ and $D_3$ span a very narrow range in absolute time (Sisson et al., 1989; Pavlis and Sisson, 1995), and recent geochronological studies (Gasser, 2010) indicate that the entire $D_2$-$D_3$ progression spanned a period of 2 m.y. or less. This narrow time span of deformation, together with the associated Border Ranges fault system to the north is the principal reason that Pavlis and Sisson (2003) first suggested that $D_2$ and $D_3$ might both be linked to strike-slip within the system in the context of the Teyssier and Cruz (2004) attachment zone model (Fig. 3A). This model suggests dominantly transcurrent motion, with an attachment layer of horizontal shear that accommodates localized shear above and a layer of evenly distributed wrench shear below. The attachment zone model was attractive to our study because it suggested an origin for the low-angle $S_2$ fabrics recognized along the western edge of the CMC, and was consistent with an observed increase in finite strain toward the gneiss transition. After the work of Pavlis and Sisson (2003), however, there were still little data on the geometry of fabrics north and west of the CMC, and it was unknown if these fabric geometries were consistent with the attachment zone model. Studies by O'Driscoll et al. (2005), O'Driscoll (2006), Pavlis et al. (2006), and Day (2007) suggested that $D_2$ fabrics in the CMC fit the geometric predictions of the attachment zone model. These studies were focused on (described here as) the Copper River, Tebay, and Bear Creek transects, and in each transect, $S_2$ appears to form a large-scale symmetric cleavage fan, centered on the Bremner River. However, in all cases the central part of this inferred fan lies within the Bremner River valley and observations in this valley were limited to scattered helicopter-supported spot observation, due to sparse rock outcrops.

Evidence for problems with applying the cleavage fan hypothesis to the CMC arose from modeling studies of O'Driscoll (2006), which used a variation on the attachment zone model as a direct comparison to observed finite strain data in the CMC. This work showed a discrepancy between predicted and observed finite strain distributions. Specifically, the attachment zone model predicts finite strain minima corresponding to the central part of a cleavage fan, yet the observed finite strain patterns were the opposite, with highest strains near the core of the shear zone. O'Driscoll (2006) suggested the finite strain pattern observed in the CMC could be explained, however, by an inverted attachment zone model where a deep strike-slip shear zone passes upward into a layer of distributed deformation (Fig. 3B). This model was testable as it made specific predictions about the structural geometry and fabric overprints to the east where the apparent cleavage fan projects toward the gneissic core, in the Fan Glacier and Bremner Glacier area.

## STRUCTURE OF THE WESTERN CMC

### Methods and Scope

Between 2003 and 2009, we conducted five summer field seasons analyzing the western termination of the CMC (Fig. 2). We conducted a total of ~175 days of fieldwork, involving five

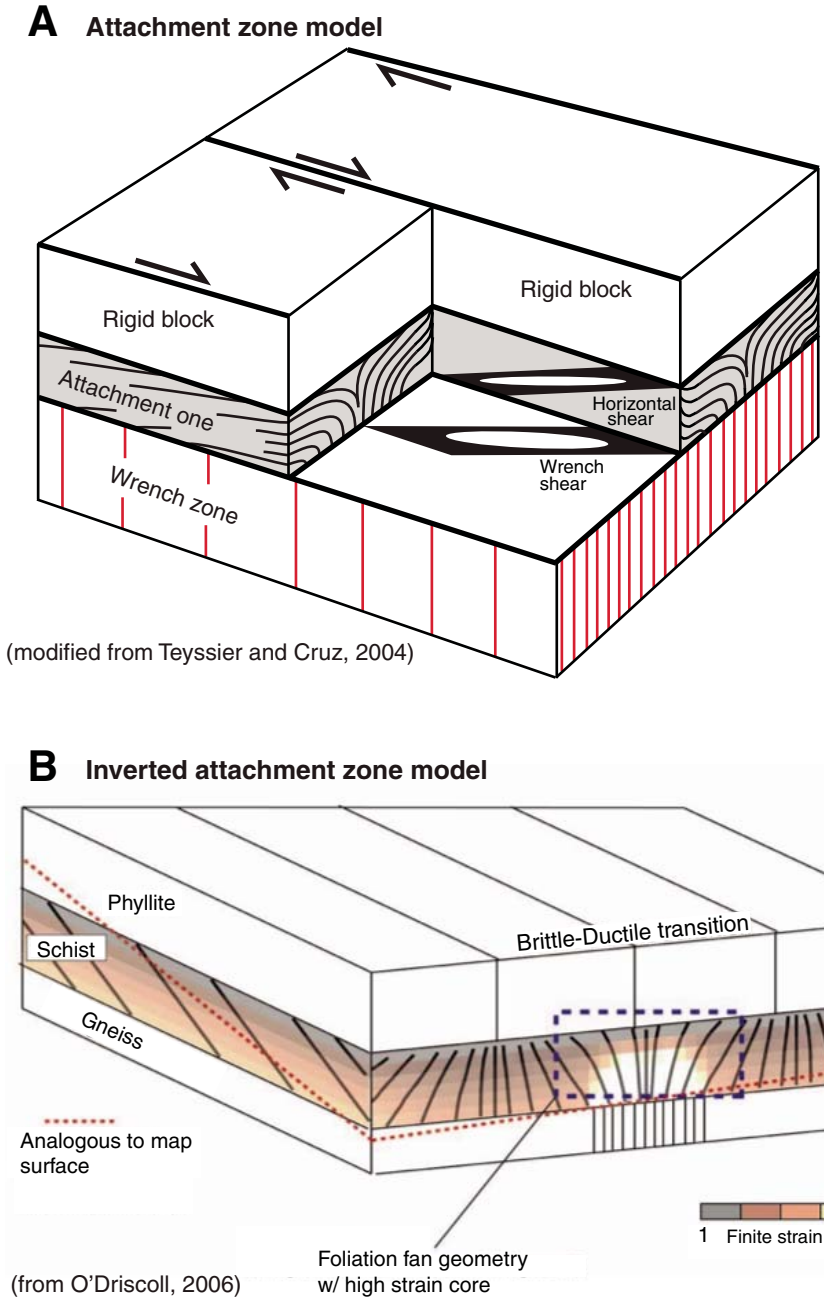


**Figure 3. Attachment zone models. (A) Attachment zone model of Teyssier and Cruz (2004). A layer of horizontal shear accommodates localized shear above and a layer of evenly distributed wrench shear below (modified from Teyssier and Cruz, 2004). (B) Inverted attachment zone model of O'Driscoll (2006). A layer of horizontal shear accommodates evenly distributed wrench shear above, and a deep localized strike-slip shear zone below.**

geologists responsible for the mapping and four assistants. This work focused on the western termination of the CMC emphasizing field mapping conducted from helicopter-placed fly camps supplemented by several full or partial days of helicopter reconnaissance filling gaps between the detailed site studies. Mapping was aided by use of a field geographic information system (GIS) that is described in detail by Pavlis et al. (2010), but this system was evolving during this project, and the GIS data files in Supplemental File 1[1] that accompany this paper show the evolution through different data formats over time. These GIS files can be used by others to recreate the geologic maps—and are best viewed by turning these data layers on and off to emphasize different structural generation—and they illustrate the power of digital maps for analyzing a structurally complex area such as this one. Our mapping includes the lithologic units of Hudson and Plafker (1982) and Pavlis and Sisson (2003), which are essentially textural divisions associated with metamorphic grade: phyllite, schist, transitional gneiss, and gneiss (Fig. 2). In addition, we systematically mapped surface traces of foliations shown as data layers in the accompanying GIS files in Supplemental File 1 [see footnote 1] (Plates 1–4). For the first three field seasons, fabric orientations were measured using traditional Brunton compasses, while electronic Geoclino compasses (produced by GSI Co.) were primarily used for the last two field seasons of mapping.

This fieldwork focused on the mapping of foliations and structures associated with multiple $D_3$ shear zones that can be traced westward from the gneissic core to the Copper River. An initial study concentrated on what Pavlis and Sisson (2003) termed the Bremner shear zone: a $D_3$ shear zone that can be traced from the gneiss core to the Copper River (Fig. 2). Mapping conducted during this project revealed the scale of the structures associated with the Bremner shear zone were far larger than suspected from earlier work, and the field work expanded to accommodate this larger scale issue. We begin here with a description of the principal structure recognized in our fieldwork, beginning in the lowest grade rocks and progressing to the gneissic core. In this section we emphasize the basic geologic relationships, which are summarized in Table 1, with our principal interpretations presented as a discussion.

[1]Supplemental File 1. Zipped file containing GIS shape file components for reconstructing map plates 1–4. If you are viewing the PDF of this paper or reading it offline, please visit http://dx.doi.org/10.1130/GES00646.S6 or the full-text article on www.gsapubs.org to view Supplemental File 1.

## Richardson Highway Transect

The western limit of the CMC metamorphism is approximately coincident with the Richardson Highway, which provides an easily accessible cross section across the bulk of the Chugach terrane (Plate 5-1; Nokleberg et al., 1989). This area was described in detail by Pavlis et al. (2003), but we summarize that study here, as it is relevant as the structurally highest part of the down-plunge extension of the CMC. Metamorphic grade throughout this transect is lower greenschist facies with sporadic development of biotite, generally limited to argillaceous layers or argillaceous metagraywackes. The Richardson Highway transect is comprised of two basic structural domains (Plate 5-1) separated by the Stuart Creek fault, a brittle fault marked by a topographic lineament that extends eastward into the center of our study area (Pavlis et al., 2003).

Domain $1^{RH}$ is characterized by steeply dipping layering and two phases of ductile deformation. The earliest fabric is a layer-parallel, steep-dipping, phyllitic pressure-solution cleavage associated with a few sparse, subisoclinal folds that are directly related to imbricate thrust systems. This thrust imbrication produces a general structural style of north-facing beds, with only localized overturning in folds related to the thrusts. This main cleavage is overprinted by a second pressure solution cleavage that is cryptic in metagraywackes but intersects the main cleavage at a low angle in argillaceous layers, typically forming a crenulation cleavage where the intersection angle exceeds ~20°. Finite strains in metagraywackes are generally constrictional with a subhorizontal stretching axis, parallel to prominent lineation, indicating that the lineation is both a stretching lineation and an intersection lineation (Pavlis et al., 2003).

North of the Stuart Creek fault (Plate 5-1), the structural style changes markedly. In this northern domain, Domain $2^{RH}$, mesoscopic folds with a south-dipping, axial planar crenulation cleavage are conspicuous over large areas (Nokleberg et al., 1989; Pavlis et al., 2003). These conspicuous folds, however, are actually $D_3$ structures (Nokleberg et al., 1989) that overprint two earlier cleavages: a layer parallel, pressure solution cleavage ($S_1$) and crenulation cleavage ($S_2$) that intersects $S_1$ at a low angle and is associated with sparse, subisoclinal folds. Nokleberg et al. (1989) correlated the two earlier cleavages to the overprints in Domain $1^{RH}$ to the south. In contrast, Pavlis et al. (2003) considered this correlation ambiguous and suggested significant strike-slip along the Stuart Creek fault had juxtaposed two assemblages with distinctly different histories. In this interpretation, $S_3$ in Domain $2^{RH}$ is probably correlative with the second fabric in Domain $1^{RH}$.

## Copper River and Bremner River Transects

Three transects were mapped across the Copper River and Bremner River valleys in the northern CMC: the West Copper River transect, the Tebay Lake transect, and the Bear Creek transect (Fig. 2; Plate 1). The geologic map and stereonet plots of fabric and structural orientation data for these transects is organized in relation to the overall structural interpretation of the Copper and Bremner River valleys, and is presented in Plate 1. Division of the data and interpretation of the overall structure are presented in the summary of this section.

### *West Copper River Canyon Transect*

The West Copper River Canyon transect examined exposures along the west bank of the Copper River canyon between the south side of the Tasnuna Valley (Ginny Creek) to the Tiekel River valley (Fig. 2). Throughout this transect the rocks are at lower to middle greenschist facies with abundant biotite in all lithologies, but neither garnet nor andalusite are observed in the meta-argillites. Two structural domains are recognized along this transect, and a third domain could be assigned to the south of the Tasnuna River where field observation is limited to one extended spot observation and aerial reconnaissance.

In Domain $1^{CR}$ between Cleeve Creek and the Tasnuna River (Plate 5-2) the structure is superficially similar to Domain 1 in the Richardson Highway transect with a predominance of steeply dipping layering and an accompanying continuous, phyllitic cleavage that is parallel to layering through large areas. However, unlike the Richardson Highway transect, this phyllitic cleavage is also axial planar to prominent upright folds that deform both layering and an older layer parallel cleavage. Upright folds in Domain $1^{CR}$ vary from close to isoclinal. Finite strains are high based on field measurements of both deformed pebble-shaped fabrics and stretch estimates from boudinaged quartz veins (O'Driscoll, 2006). Boudinage and pebble shapes also demonstrate that a prominent, subhorizontal, approximately east-west–trending lineation represents the maximum stretching axis. This is similar to that observed elsewhere in both the Richardson Highway transect and the western CMC as a whole (e.g., Pavlis and Sisson, 2003).

Domain $2^{CR}$ comprises the region between Cleeve Creek and the area just south of the Tiekel River (Plate 5-2). Similar structures could be present in the Tiekel River valley, but based on

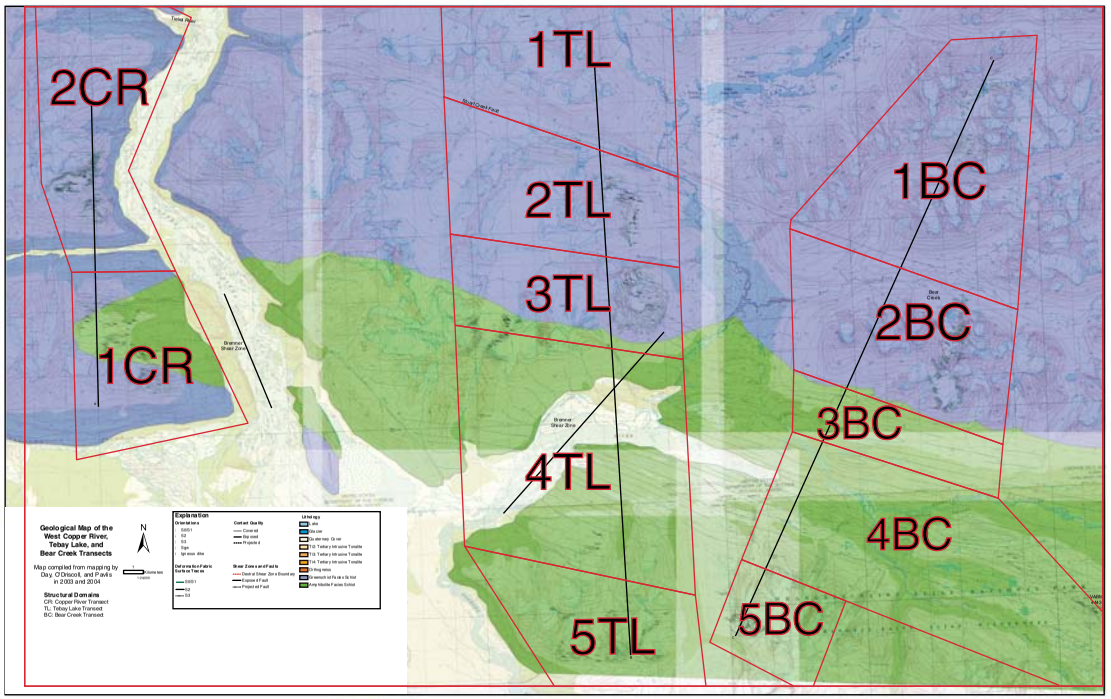


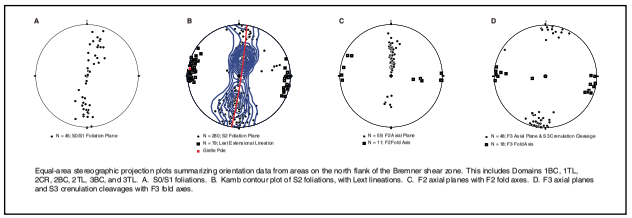


Equal-area stereographic projection plots summarizing orientation data from areas on the north flank of the Bremner shear zone. This includes Domains 1BC, 1TL, 2CR, 2BC, 2TL, 3BC, and 3TL. A. S0/S1 foliations. B. Kamb contour plot of S2 foliations, with Lext lineations. C. F2 axial planes with F2 fold axes. D. F3 axial planes and S3 crenulation cleavages with F3 fold axes.

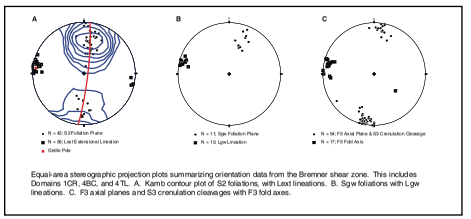


Equal-area stereographic projection plots summarizing orientation data from the Bremner shear zone. This includes Domains 1CR, 4BC, and 4TL. A. Kamb contour plot of S2 foliations, with Lext lineations. B. Sgw foliations with Lgw lineations. C. F3 axial planes and S3 crenulation cleavages with F3 fold axes.

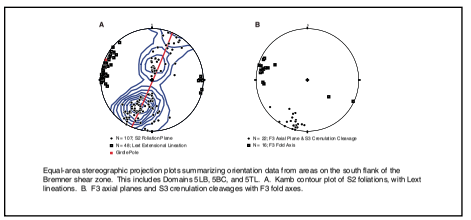


Equal-area stereographic projection plots summarizing orientation data from areas on the south flank of the Bremner shear zone. This includes Domains 5LB, 5BC, and 5TL. A. Kamb contour plot of S2 foliations, with Lext lineations. B. F3 axial planes and S3 crenulation cleavages with F3 fold axes.

**Plate 1. Copper River and Bremner River geologic map and stereographic projection plots of orientation data. Layer of structural domain boundaries layer can be turned on and off in this file. If you are viewing the PDF of this paper or reading it offline, please visit http://dx.doi.org/10.1130/GES00646.S1 or the full-text article on www.gsapubs.org to view the full-sized PDF file of Plate 1.**

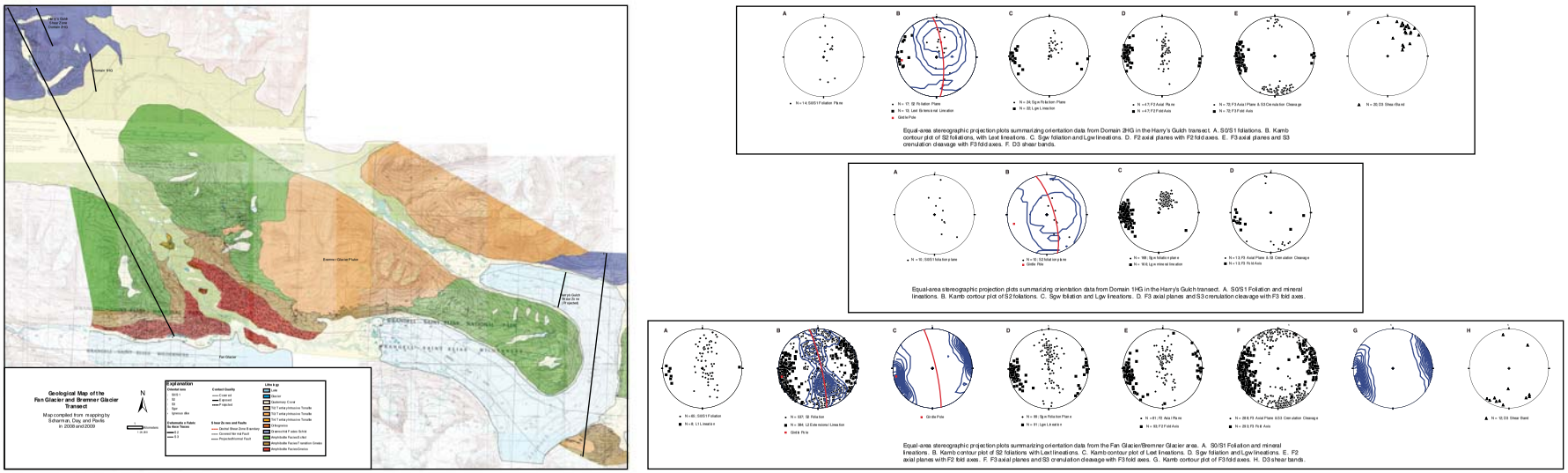


**Plate 2. Harry's Gulch, Fan Glacier, Bremner Glacier geologic map, and stereographic projection plots of orientation data. If you are viewing the PDF of this paper or reading it offline, please visit http://dx.doi.org/10.1130/GES00646.S2 or the full-text article on www.gsapubs.org to view the full-sized PDF file of Plate 2.**

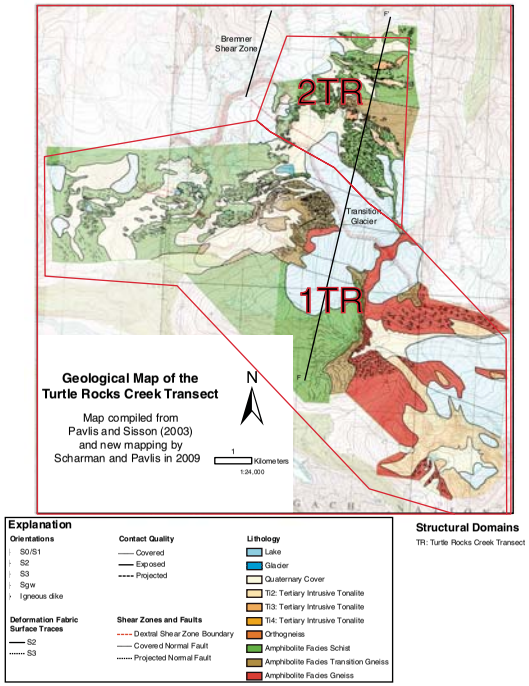


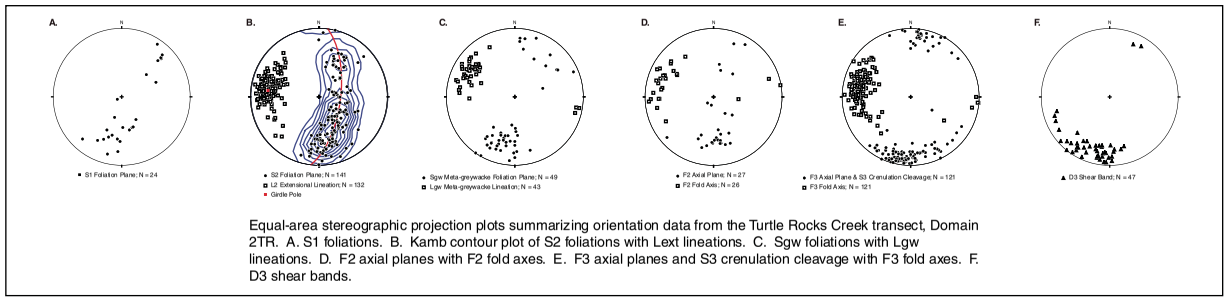


Equal-area stereographic projection plots summarizing orientation data from the Turtle Rocks Creek transect, Domain 2TR. A. S1 foliations. B. Kamb contour plot of S2 foliations with Lext lineations. C. Sgw foliations with Lgw lineations. D. F2 axial planes with F2 fold axes. E. F3 axial planes and S3 crenulation cleavage with F3 fold axes. F. D3 shear bands.

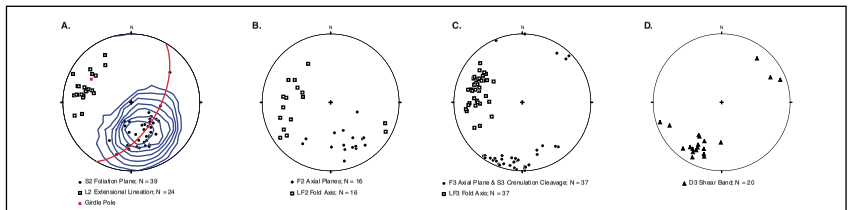


Equal-area stereographic projection plots summarizing orientation data from the Turtle Rocks Creek transect, Domain 1TR. A. Kamb contour plot of S2 foliations with Lext lineations. B. F2 axial planes with F2 fold axes. C. F3 axial planes and S3 crenulation cleavage with F3 fold axes. D. D3 shear bands.

**Plate 3. Turtle Rocks Creek geologic map and stereographic projection plots of orientation data. Layer of structural domain boundaries layer can be turned on and off in this file. If you are viewing the PDF of this paper or reading it offline, please visit http://dx.doi.org/10.1130/GES00646.S3 or the full-text article on www.gsapubs.org to view the full-sized PDF file of Plate 3.**

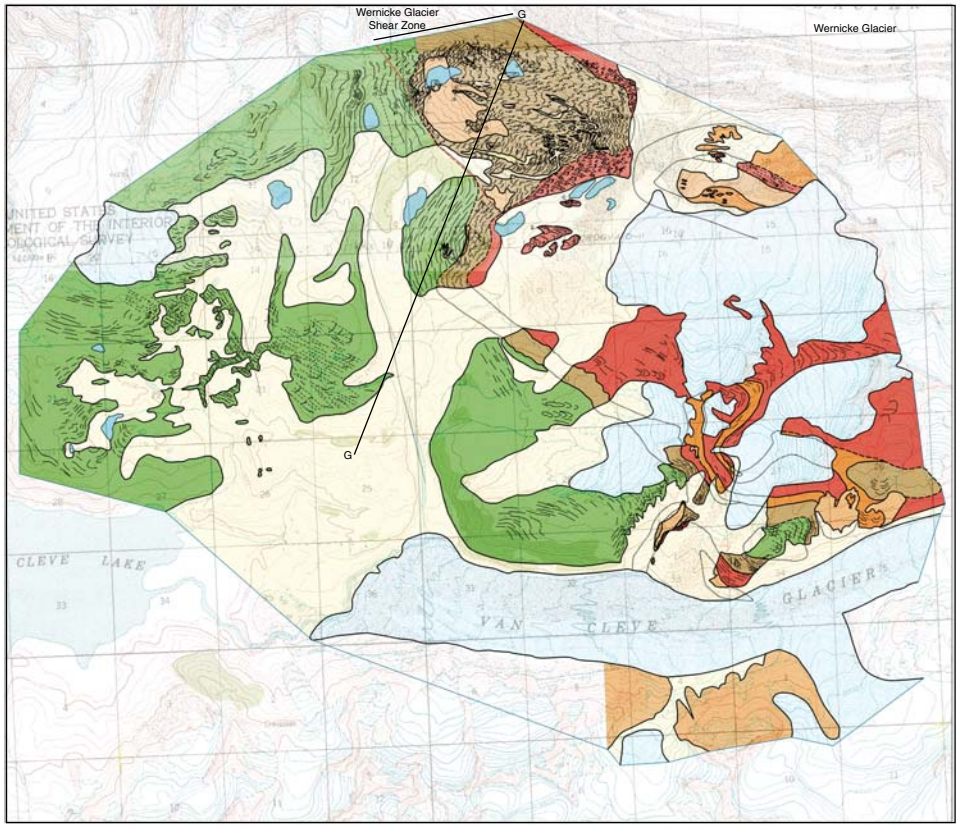


**Geological Map of the Wernicke Glacier Transect**

Map compiled from Pavlis and Sisson (2003) and new mapping by Scharman and Pavlis in 2008

N

1 Kilometers

1:24,000

**Explanation**

**Orientations**
- S0/S1
- S2
- S3
- Sgw
- Igneous dike

**Deformation Fabric Surface Traces**
- S2
- S3

**Contact Quality**
- Covered
- Exposed
- Projected

**Shear Zones and Faults**
- Dextral Shear Zone Boundary
- Covered Normal Fault
- Projected Normal Fault

**Lithology**
- Lake
- Glacier
- Quaternary Cover
- Ti2: Tertiary Intrusive Tonalite
- Ti3: Tertiary Intrusive Tonalite
- Ti4: Tertiary Intrusive Tonalite
- Orthogneiss
- Amphibolite Facies Schist
- Amphibolite Facies Transition Gneiss
- Amphibolite Facies Gneiss

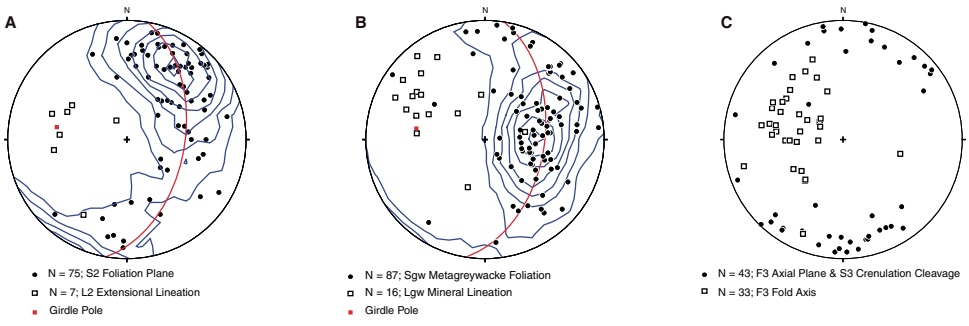


Equal-area stereographic projection plots summarizing orientation data from the Wernicke Glacier transect. A. Kamb contour plot of S2 foliations, with Lext lineations. B. Kamb contour plot of Sgw foliations, with Lgw lineations. C. F3 axial planes and S3 crenulation cleavage with F3 fold axes.

**Plate 4. Wernicke Glacier geologic map and stereographic projection plots of orientation data. Layer of structural domain boundaries layer can be turned on and off in this file. If you are viewing the PDF of this paper or reading it offline, please visit http://dx.doi.org/10.1130/GES00646.S4 or the full-text article on www.gsapubs.org to view the full-sized PDF file of Plate 4.**

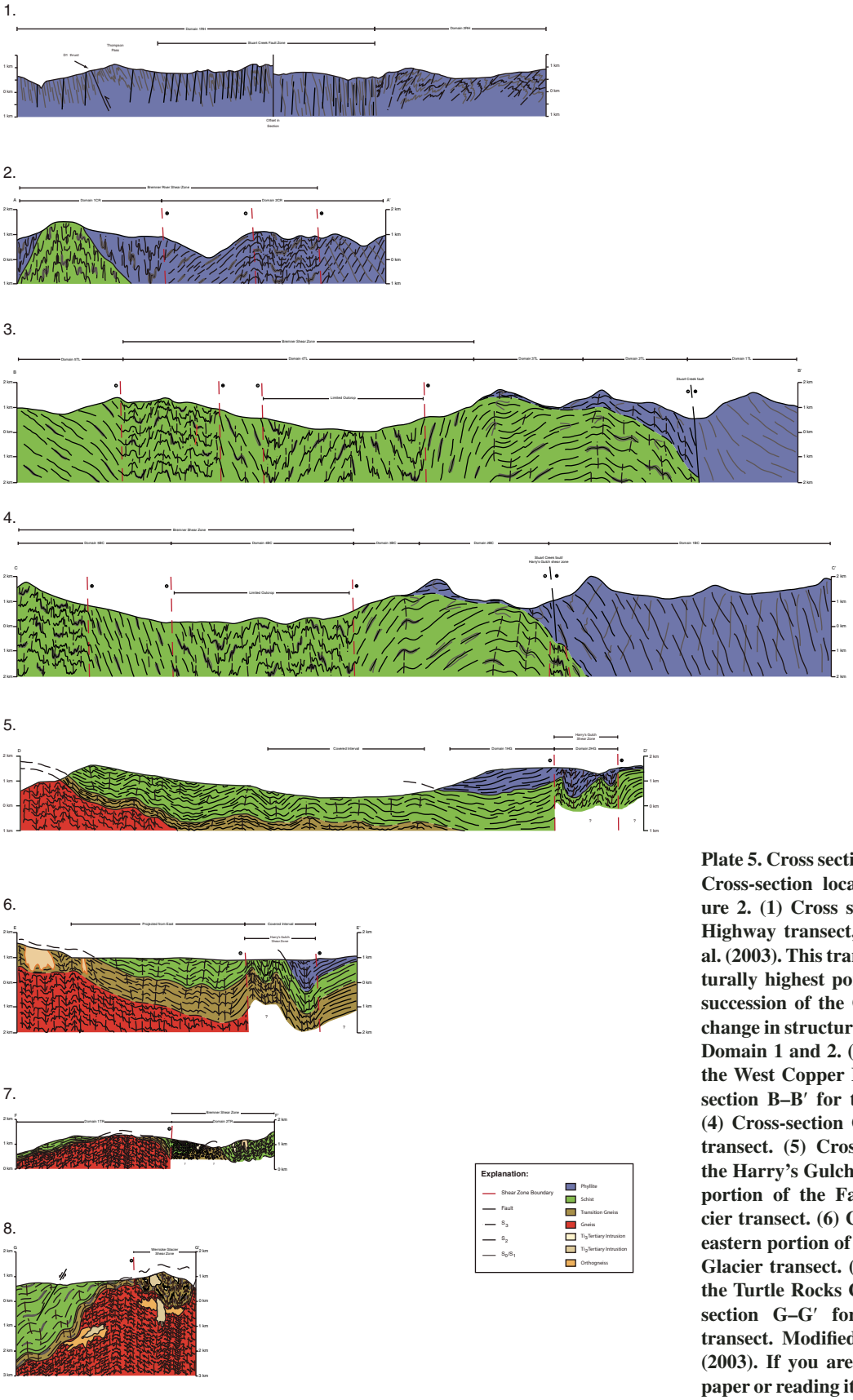


**Plate 5. Cross sections for the western CMC. Cross-section locations are shown in Figure 2. (1) Cross section of the Richardson Highway transect, modified from Pavlis et al. (2003). This transect represents the structurally highest portion of the down-plunge succession of the CMC. Note the dramatic change in structural characteristics between Domain 1 and 2. (2) Cross-section A–A′ for the West Copper River transect. (3) Cross-section B–B′ for the Tebay Lake transect. (4) Cross-section C–C′ for the Bear Creek transect. (5) Cross-section D–D′ spanning the Harry's Gulch transect and the western portion of the Fan Glacier/Bremner Glacier transect. (6) Cross-section E–E′ for the eastern portion of the Fan Glacier/Bremner Glacier transect. (7) Cross-section F–F′ for the Turtle Rocks Creek transect. (8) Cross-section G–G′ for the Wernicke Glacier transect. Modified from Pavlis and Sisson (2003). If you are viewing the PDF of this paper or reading it offline, please visit http://dx.doi.org/10.1130/GES00646.S5 or the full-text article on www.gsapubs.org to view the full-sized PDF file of Plate 5.**

overflights and comparison with areas immediately along strike, there are almost certainly other structural complexities in the Tiekel River valley. In Domain $2^{CR}$, finite strains appear to be lower than Domain $1^{CR}$, and the relationships between fabrics and layering are very different. Specifically, layering and an accompanying layer parallel foliation show a general north dip at low to moderate angles, but both layering and the older fabric are overprinted by a prominent, moderately to steeply south-dipping crenulation cleavage. This crenulation cleavage is axial planar to mesoscopic folds that are upright to steeply inclined, horizontal to gently plunging folds. Unlike the subisoclinal to isoclinal folds of Domain $1^{CR}$, these folds are more open, with interlimb angles of 60°–90°, and show enveloping surfaces that define the general north dip of layering.

These observations indicate that in both Copper River Domains the rocks carry a two phase deformational history: (1) An early phase produced the layer parallel cleavage, although no prominent folds were seen in association with this fabric, and (2) this cleavage was overprinted by conspicuous fold structures throughout the transect with upright to steeply inclined axial surfaces and an associated steeply dipping, axial planar crenulation cleavage. Geometrically, the younger cleavages form vertical dips throughout Domain $1^{CR}$ and moderate to steep south dips in Domain $2^{CR}$ (Plate 5-2). Moreover, based on fold styles that range from isoclinal to tight from south to north, it also appears that finite strains associated with this folding decrease from south to north.

Although these overprints are clear from field relationships, it is not clear how this two-phase deformation history correlates to adjacent areas. Based on overprinting alone, the history seemingly is closely analogous to the Domain $1^{RH}$ in the Richardson Highway transect. However, there is an important difference in that upright folds are conspicuous throughout the Copper River transect, and these folds define a low to moderate dip angle of enveloping surfaces. This observation suggests that layering had a relatively low dip prior to the younger deformation, which is very different from the Richardson Highway where it appears layering was steeply dipping prior to the superimposed, younger cleavage (e.g., Pavlis et al., 2003). Immediately to the east of Domains $1^{CR}$ and $2^{CR}$, however, a prominent low-angle fabric ($S_2$) is mapped throughout the CMC, and this fabric is associated with the main continuous cleavage that is generally parallel to layering due to $D_2$ isoclinal folding. Thus, carrying the geometric elements of the CMC overprints westward to the Copper River suggests that the early, layer-parallel cleavage was $S_2$ and the prominent overprinting crenulation cleavage is a $D_3$ structure—$S_3$. Based on these observations and the relationships described below, structures in the West Copper River transect are part of the CMC, and are distinctly different than the structures in the Richardson Highway transect.

### *Tebay Lake Transect*

This transect extends from just north of the Stuart Creek fault, near Tebay Lake, southward across the Bremner River and into the northwestern part of the CMC (Fig. 2; Plate 1). Metamorphic grade varies markedly across this transect from the lower greenschist facies assemblage chlorite ± biotite in meta-argillites near the Stuart Creek fault to upper greenschist facies assemblages biotite + andalusite ± garnet to the south. Accompanying these changes in grade are major changes in structural style and orientation across this transect.

At the northern end of this transect (Plate 5-3), Domain $1^{TL}$ is characterized by homoclinal, steeply dipping layering with a corresponding steeply dipping foliation subparallel to layering. Within this domain, assignment of structural generation is not straightforward because the rocks are dominantly metagraywackes that show only a single fabric that we interpret as a finite strain fabric ($S_{gw}$), which is equivalent to the $D_2$ fabric in this domain. Based on other observations just to the east, and overprints recognized immediately to the south, we suggest this domain is dominated by $D_3$ strain related to dextral shear along the Stuart Creek fault.

Domain $2^{TL}$ in this transect extends from ~1 km south of the Stuart Creek fault to Porcupine Creek (Plate 5-3). This domain contains three readily distinguished fabrics, all of which have associated folds. Since all three generations of structure can be distinguished within Domain $2^{TL}$ and none of the fold systems transposes earlier structure, generalization of the structure is difficult, but the cross section in Plate 5-3 shows a generalized conception. Specifically, the earliest $D_1$ structures are a layer-parallel foliation that is locally associated with small-scale, subisoclinal folds, but generally is not associated with conspicuous mesoscopic structure. This cleavage and layering are conspicuously folded along tight to subisoclinal, gently inclined to recumbent, horizontal to gently west plunging folds. These folds are associated with a conspicuous axial planar crenulation cleavage ($S_2$). $D_2$ structures also show a marked variation in style across strike within this domain from tight to close folds in the north to subisoclinal folds at the transition to Domain $3^{TL}$ in Porcupine Creek. This observation strongly suggests a $D_2$ finite strain gradient across this domain with higher strains in the south. Finally, $S_2$ is variably overprinted by a series of open to tight, horizontal to gently west-plunging upright folds (Fig. 4D). $D_3$ is associated with a steeply dipping crenulation cleavage that overprints both the $S_2$ cleavage and the $S_1$ cleavage in argillaceous rocks. Metagraywackes within this domain do not show overprinting cleavages and typically show only one fabric—$S_{gw}$—with a poorly developed foliation and a prominent, subhorizontal, east-west–trending lineation ($L_{gw}$). We interpret this metagraywacke fabric as a finite strain fabric.

South of Porcupine Creek and extending westward at least 12 km along strike is Domain $3^{TL}$ (Plate 5-3), which is characterized by a dominance of $D_2$ fabrics. Throughout Domain $3^{TL}$, horizontal to gently west plunging $D_2$ folds are subisoclinal to isoclinal with $S_1$ and $S_0$ transposed into $S_2$ foliation. $S_2$ is horizontal to gently south dipping throughout the bulk of this domain, but rolls to moderate south dips in the transition to Domain $4^{TL}$. $D_3$ structures are conspicuously absent or limited to open flexures in the $S_2$ foliation, with sporadic development of steeply dipping $S_3$ crenulation cleavage overprinting $S_2$ (Fig. 4D). In cross section, this domain, together with Domain $2^{TL}$ comprises what we term a $D_2$ flat belt, characterized by subhorizontal $S_2$ foliation that rolls into steeper dips southward; either representing a macroscopic $D_3$ fold or $D_2$ foliation fan. Mesoscopic shear-sense indicators are not well developed and are limited to a few asymmetric boudins suggesting top to the west shear.

As $S_2$ dips steepen southward, Domain $4^{TL}$ is defined as rocks with $S_2$ dips greater than 50°. In this definition, Domain $4^{TL}$ extends at least 8 km across strike to the Bremner River, and based on helicopter reconnaissance in the Bremner River lowlands this domain may extend as much as 2 km farther south. Throughout this domain the rocks are characterized by one dominant continuous cleavage—$S_2$—that overprints an earlier layer-parallel mica foliation, and appears to be a direct continuation of the monoclinal rollover of Domain $3^{TL}$. $D_3$ overprints are present within this domain but are cryptic because the $S_2$ foliation has rotated and become parallel with $D_3$ foliation, an issue discussed later in this paper. Finite strains appear to be high within this domain based on local object strains as well as stretches inferred from boudinaged quartz veins (O'Driscoll, 2006). Shear-sense indicators are limited to asymmetric boudins, which indicate dextral shear during the main deformation across this zone.

Domain $5^{TL}$ represents the southern edge of this transect, and is a higher grade, mirror image of Domain $3^{TL}$. That is, $S_2$, the dominant continuous cleavage in Domain $5^{TL}$ based on correlations to Pavlis and Sisson (2003), rolls from the steep dips of Domain $4^{TL}$ into a southern flat belt

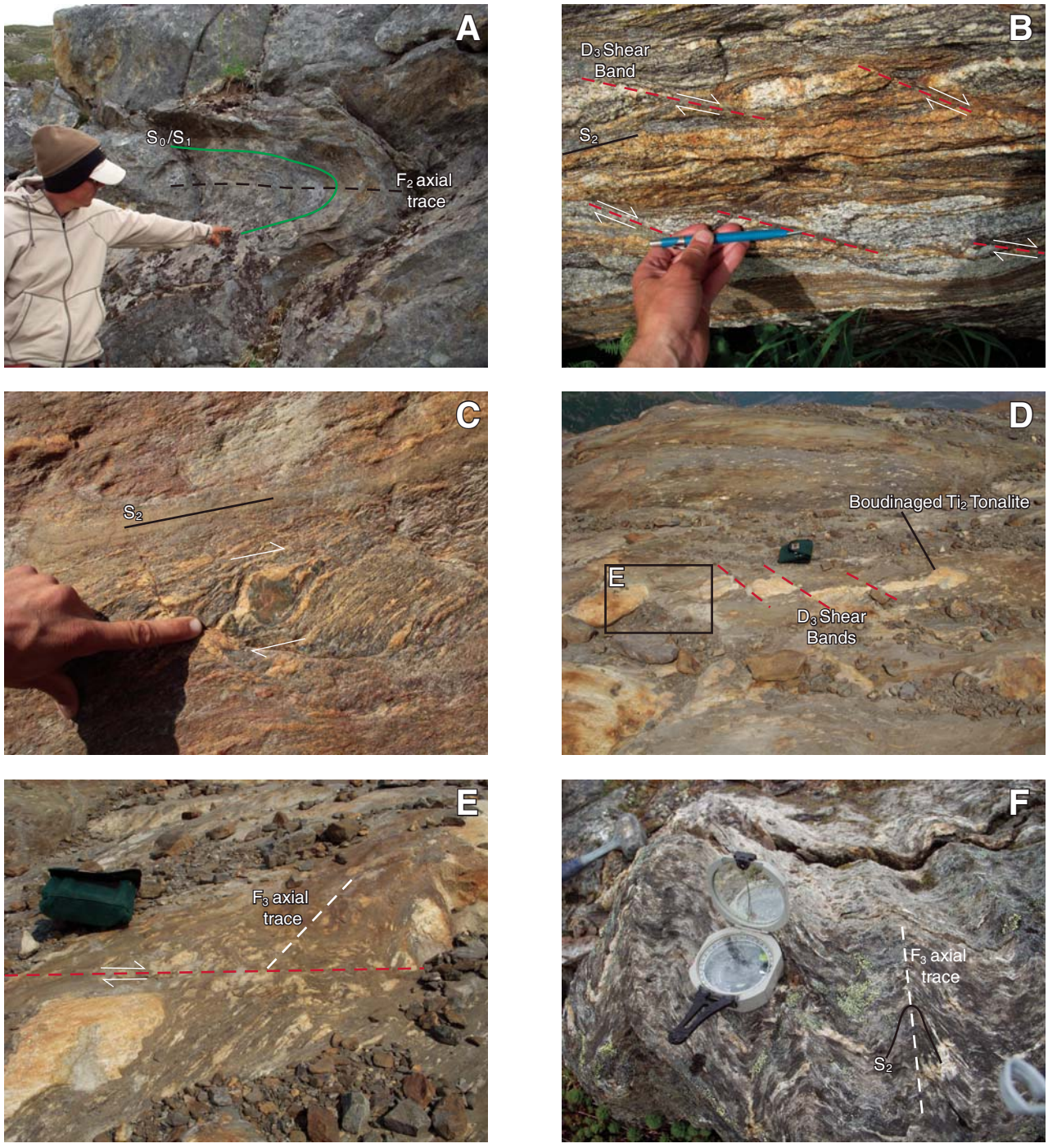


**Figure 4. Field photographs of geologic structures throughout the CMC transects. (A) Large, recumbent, tight $D_2$ fold deforming older $S_0/S_1$ foliation in the Fan Glacier/Bremner Glacier transect. (B) $D_3$ shear bands in the transition gneiss at Fan Glacier/Bremner Glacier showing dextral offset of older $S_2$ foliation and $Ti_2$ tonalite intrusives. (C) Cordierite σ clast displaying top-to-the-east shear sense in the transition gneiss in the Turtle Rocks Creek transect. (D) Large $D_3$ shear bands displaying dextral shear sense within the Bremner shear zone, and a boudinaged $Ti_2$ tonalite intrusion. Inset box shows location of image E. (E) $F_3$ axes truncated against an individual $D_3$ shear band, suggesting that these are folds formed by wrenching motion. (F) Tight, upright folds, representative of $F_{3AP}$ within the $D_3$ dextral shear zones in the Wernicke Glacier shear zone.**

and becomes nearly flat lying with a gentle west dip. As in other parts of the CMC, this flat $S_2$ foliation is locally deformed by $D_3$ shear zones with localized $S_3$ fabric development and dextral shear bands.

Lineations across the Tebay Lake transect are subhorizontal to shallowly west plunging, and invariably represent both an extension and intersection lineation consistent with type 3 fold interference patterns among the fold generations. Lineation trends, however, show a significant spatial variation across the transect. To the north of Domain $4^{TL}$, lineations have an average east-west trend, parallel to strike in the steeply dipping rocks of Domain $4^{TL}$ (Fig. 4B) but become more northwest trending south of the Bremner river (Fig. 5A).

***Bear Creek Transect***

The fourth transect across this region crosses several unnamed drainages, but is referred to here as the Bear Creek transect (Fig. 2; Plate 1). The Bear Creek transect includes mapping of a significant area north of the Stuart Creek fault across the Bremner River into high-grade gneissic rocks in the core of the CMC. Metamorphic grade is low, however, in most of this transect with amphibolite facies assemblages limited to within 3–4 km of the gneissic core. This relatively narrow high-grade zone is common along the northern edge of the CMC and is typically associated with steeply dipping isograds (e.g., Pavlis and Sisson, 1995, 2003). The origin of the steeply dipping isograds is unclear but probably relates to $D_3$ structural history, either differential exhumation or compression of isograds by $D_3$ strain (e.g., as suggested by Gasser et al. [2011] for syn-$D_2$ metamorphism).

North of the Stuart Creek fault, in Domain $1^{BC}$ (Plate 5-4), the structural style is completely different than the closest analogous site we have examined in detail, along the Richardson Highway. In the Bear Creek transect, layering generally dips steeply southward with north-facing tops, and similar structure extends nearly to the trace of the Border Ranges fault. Layering and an early, layer-parallel chlorite-white mica foliation are overprinted by a steeply north-dipping foliation—$S_2$ (Fig. 4B). South of the Stuart Creek fault, the Bear Creek transect is indistinguishable from the general structure of the Tebay transect. In Domain $2^{BC}$, within ~1 km of

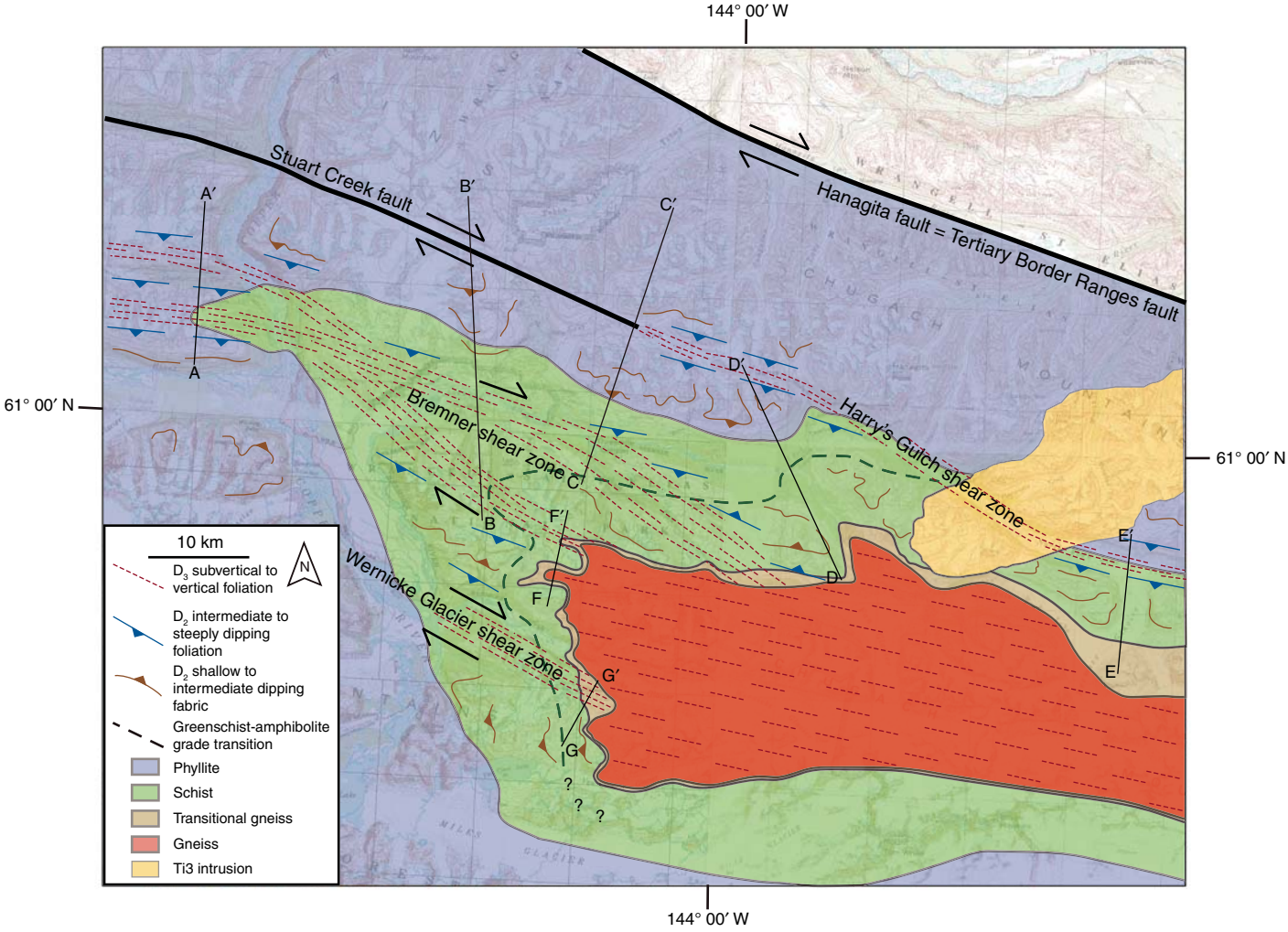


**Figure 5. Regional overview geologic map of the western Chugach metamorphic complex. Geologic contacts and isograds modified from Hudson and Plafker (1982) and Richter et al. (2005). The main structure in the region is the $D_3$ Bremner shear zone. This is a dextral slip shear zone, which exhibits an anastamosing structure with several lenses exhibiting relatively low finite strains, and subvertical to vertical $D_3$ structures. Other prominent $D_3$ dextral shear zones in the region are the Wernicke Glacier shear zone and Harry's Gulch shear zone, the continuation of the brittle Stuart Creek fault into the ductile deformation domain. Between these shear zones are relatively rigid blocks of shallowly to steeply dipping $D_2$ foliations.**

the Stuart Creek fault (Plate 5-4), steeply dipping layering and foliation equivalent to Domain $1^{TL}$ pass southward into a complex overprinting zone where three phases of deformation are superimposed, the equivalent of Domain $2^{CR}$. As in the Tebay transect, in Domain $3^{BC}$, $D_2$ folds tighten southward and ultimately become isoclinal (equivalent to Domain $3^{TL}$). $D_2$ axial planar foliations ($S_2$) show a gentle south dip throughout Domains $2^{BC}$ and $3^{BC}$ until just north of the Bremner River canyon where they roll to steeper dips; analogous to the southern limit of Domain $3^{TL}$ in the Tebay transect.

Based on this analogy with the Tebay transect, aerial reconnaissance, aerial photograph interpretation, and from field observations near Vertical Angle Benchmark 4443, we infer that the structure in the Bremner River lowlands is equivalent to Domain $4^{LB}$ with a steeply dipping dominant foliation, and we term this as Domain $4^{BC}$ (Plate 5-4). Nonetheless, observations at this camp, as well as observations farther east (see below) suggest that more complex overprints are present within this steep zone, including localized zones of high $D_3$ strain recognized as crenulation overprints and shear bands.

Finally, to the south, in Domain $5^{BC}$ (Plate 5-4) the structure is similar to Domain $5^{TL}$ in the Tebay transect with a distinct north-dipping continuous $S_2$ cleavage, rolling to lower dips southward. Unlike the Tebay transect, however, $S_2$ foliation at the southern end of the Bear Creek transect never rolls to nearly flat dips, but instead north-dipping $S_2$ foliation continues structurally downward across the schist-gneiss transition, where $D_3$ overprints become significant and $D_2$ structure is difficult to infer from aerial reconnaissance.

### *Copper River and Bremner River Transects Summary*

Domains that include the West Copper River Canyon, Tebay, and Bear Creek transects can be divided into three separate groups with similar structural geometries and fabric orientations. In particular, $D_2$ fabric domains can be readily divided spatially into what we term as flat-belt domains, where $S_2$ foliation generally dips <50°, and steep zones where $S_2$ foliation generally dips >50°. Similarly, variations in $D_3$ strain are also mappable by variations in fold styles and intensity of the $D_3$ fabrics. $S_2$ foliation in Domains $2^{CR}$, $1^{LB}$, $2^{LB}$, $3^{LB}$, $1^{BC}$, $2^{BC}$, and $3^{BC}$ predominantly dips southward at shallow to intermediate angles, and comprises a mappable flat belt on the north side of the Bremner River canyon. Domains $5^{LB}$ and $5^{BC}$ on the south side of the Bremner River canyon are similar to the domains on the north side of the canyon, except that $S_2$ dips predominantly to the north, and we group these domains as a southern flat-belt region. Domains $1^{CR}$, $4^{LB}$, $4^{BC}$, and $2^{TR}$ are located between the two flat-belt regions; have steeply dipping $S_2$ and $S_{gw}$ foliation; are deformed into tight, upright $D_3$ folds; and are grouped into a central steep belt. This steep belt is interpreted as being a large $D_3$ shear zone that separates the two adjacent $D_2$ flat belts to the north and south.

## Harry's Gulch Transect

Rocks in the Harry's Gulch transect (Fig. 2) are greenschist facies schist, analogous to the extreme northern ends of the Tebay and Bear Creek transects. Within this map area, two distinct structural domains are recognized: a low-finite strain region in the south, and a higher-finite strain area that occupies Harry's Gulch. The geologic map and stereonet plots of orientation data for the Harry's Gulch transect are presented in Plate 2.

In Domain $1^{HG}$ (Plate 5-5), the rocks are predominantly metagraywacke with limited, thin argillaceous and chloritic schist layers. Metagraywacke foliation—$S_{gw}$—has a uniform, shallow to intermediate southwest dip. Layering ($S_0/S_1$) and $S_2$ foliations are not often observed in Domain $1^{HG}$, but both have a similar shallow to intermediate dip. Mineral lineations—$L_{gw}$—are clear in the metagraywacke and are shallowly plunging to the west-southwest. $D_3$ structures are minimal in the southern Harry's Gulch map area, and are limited to the thin, argillaceous schist layers. $D_3$ structures are upright, horizontal to shallowly west plunging, open folds ($F_{3AP}$) with no associated axial planar cleavage. $D_3$ folds in Domain $1^{HG}$ have a wavelength of approximately half a meter or less. In cross section, some mesoscopic $D_3$ structures are apparent, but are large wavelength, open folds (Plate 5-5). A few C′ shear bands cut $S_{gw}$. These shear bands are associated with boudinaged and folded quartz veins indicating a dextral shear sense, and asymmetric boudinaged quartz veins showing top-to-the-east shear sense.

Structures indicative of a high $D_3$ finite strain are observed in Domain $2^{HG}$ (Plate 5-5). Within a distance of ~100 m, the uniformly southwest-dipping foliation of the metagraywackes in Domain $1^{HG}$ is deformed into conspicuous $D_3$ folds, at mesoscopic scale. $D_3$ structures are upright, horizontal to gently west plunging, closed to tight folds, with steep to vertical axial planes. $D_2$ structures observed in Domain $2^{HG}$ are inclined to recumbent, horizontal to gently west-plunging, tight folds ($F_{2AP}$, $L_{F2}$), with a shallow- to intermediate-dipping axial planar cleavage ($S_2$). $F_{2AP}$ and $S_2$ are clearly refolded by $D_3$, forming type 3 fold interference patterns. $L_{ext}$ observed on $S_2$ foliation planes are uniform, plunging shallowly to the west. $S_{gw}$ and $L_{gw}$ orientations within the high strain zone are oriented similarly to those outside of this zone.

$D_3$ dextral C′ shear bands are pervasive throughout Domain $2^{HG}$. These shear bands have an average southeast strike and intermediate to steep, southwest dip, and deform $S_2$ foliations. $D_3$ fold axes are oblique to the shear bands. We infer these $D_3$ folds were formed in response to wrenching motion in Domain $2^{HG}$, but could also reflect the pure shear shortening component of transpression. The presence of abundant dextral shear bands, accompanying $D_3$ wrench folds, and higher finite strains than in Domain $1^{HG}$ suggests that Domain $2^{HG}$ is a previously unmapped, dextral, $D_3$ shear zone, referred to here as the Harry's Gulch shear zone (Plate 5-5). An anastomosing map pattern is apparent for the Harry's Gulch shear zone, as a small lens of undeformed, metagraywacke is observed within the shear zone boundaries between smaller zones of dextral shearing. Previous workers (e.g., O'Driscoll, 2006; Day, 2007) have projected the proposed Stuart Creek fault—a brittle, dextral slip fault—into this valley, and have suggested this feature has ~100 km of offset. Thus, we interpret that the Harry's Gulch shear zone is the extension of the Stuart Creek fault to depths below the brittle-ductile transition within the CMC (Plate 5-5).

## Fan Glacier/Bremner Glacier Transects

The Fan Glacier/Bremner Glacier transects represent a broad map area covering the upper amphibolite gneiss core, across the transition gneiss, into the amphibolite facies schist of the CMC (Fig. 2). This mapped region represents one of the best exposures of deformation in the areas where $D_3$ shear zones merge with the gneiss core. The geologic map and stereonet plots of fabric and structural orientation data for the Fan Glacier/Bremner Glacier area are presented in Plate 2. Cross sections displaying the overall structure described in this section are presented for both the western portion (Plate 5-5) and the eastern portion (Plate 5-6) of this transect.

The dominant fabric throughout the Fan Glacier/Bremner Glacier map area is a continuous cleavage representing a mica foliation—$S_2$—in pelitic rocks and a composite shape fabric/mica foliation ($S_{gw}$) in metagraywackes. $S_2$ is axial planar to $D_2$ folds, which are tight to isoclinal, recumbent to gently inclined folds ($F_{2AP}$, $L_{F2}$). $L_{ext}$ and $L_{gw}$ lineations are observed on $S_2$ and $S_{gw}$ cleavage planes in the amphibolite facies schist and vary between shallowly southwest, west, east, and northeast plunging. $D_2$ structures are moderately inclined, horizontal to gently west-plunging

folds ($F_{2AP}$, $L_{F2}$), with moderately north- and south-dipping axial surfaces (Fig. 4A). $D_2$ folds are generally observed in the argillaceous-rich schist layers. $F_{2AP}$ and associated $S_2$ cleavage are refolded by $D_3$ folds ($F_{3AP}$) forming type 3 interference fold patterns. $D_3$ folds are typically upright, horizontal to gently west-plunging, open folds. $D_3$ folds in the amphibolite facies schist are large—varying between 10's of meters to 1 or 2 km in wavelength.

Long wavelength $D_3$ folds, similar to those observed in the schist, are observed in the transitional gneiss. However, smaller, parasitic $D_3$ folds—on the order of a few meters to centimeters in wavelength—are more common within the transitional gneiss. $D_3$ folds in the transitional gneiss are also upright, open, and horizontal to gently east and west plunging ($F_{3AP}$). Two helicopter spot checks in the Middle Bremner River valley constrain the location of the transitional gneiss-schist contact. From this mapping, it is clear that, although folded, the transitional gneiss-schist contact V's to the north in the Middle Bremner River valley, indicating that the transitional gneiss-schist contact has a gentle northward dip in this part of the northern CMC (Plates 5-5 and 5-6).

The northern edge of the gneiss core of the CMC is extensively exposed in this area from Fan Glacier on the west to Bremner Glacier on the east. Within the gneiss, $D_3$ is the dominant structure observed. Unlike those observed in the overlying transitional gneiss and schist, $D_3$ structures in the gneiss are upright, gently west-plunging, close to tight folds. $D_3$ also deforms older $S_2$ and $F_{2AP}$ into type 3 fold interference patterns. $D_3$ folds in the gneiss are pervasive at smaller scales, with wavelengths of ~5 m or less, and are not parasitic folds on the flanks of larger structures, unlike the larger mesoscopic scale structures observed in the overlying transitional gneiss and amphibolite grade schist layers.

At map scale, the gneiss transition in the Fan Glacier/Bremner Glacier region shows significant variations along strike (Fig. 2). To the west, in the Fan Glacier area the gneiss transition dips moderately northward from the Turtle Rocks creek map area (Fig. 2) to the Bremner River where it flattens to low-dip to produce the dramatic V in the outcrop trace. Throughout this area, however, the transitional gneiss unit is relatively uniform in thickness. To the east of the Bremner River, the transitional gneiss maintains a similar thickness but returns to moderate north dips, but with a distinct change in strike (Plates 2 and 5). When it re-emerges from ice cover east of the Bremner Glacier, however, the transition gneiss occupies a broad band of moderately north-dipping rocks and represents a distinctly thicker transition gneiss. The origin of these along strike variations is uncertain, but may be related to pluton emplacements or compositional variations across the gneiss transition along strike.

Shear sense indicators are relatively common in the Fan Glacier/Bremner Glacier map area and provide constraints on the kinematics of both $D_2$ and $D_3$. In flat lying $S_2$ foliation domains of the transitional gneiss and schist, asymmetric quartz boudins and σ-type objects are observed in planes perpendicular to $S_2$ and parallel to $L_{ext}$. These shear sense indicators display a top-to-the-east shear direction. The other prominent shear sense indicators are a series of dextral C′ shear bands, which are also observed in the gneiss core as well as the transitional gneiss and schist (Fig. 4B). These dextral shear bands dip steeply to the north, and are $D_3$ structures because they crosscut and fold the shallow-dipping $S_2$ foliations.

Two generations of tonalite intrusions are present in the Fan Glacier/Bremner Glacier map area. Smaller intrusions are observed parallel to $S_2$ foliations, and are relatively widespread throughout the transition gneiss in this map region. These are syn-$D_2$ plutons, as the intrusions have foliations with similar orientation to $S_2$, and are deformed by $D_3$ folding and dextral shear bands. A large intrusion is observed in the central part of the mapped area (Fig. 2) and is shown on regional maps (e.g., Richter et al., 2005). This pluton has a mesoscopic biotite foliation, presumably solid-state, that is steeply dipping, consistent with the orientation of the $F_{3AP}$ in adjacent rocks, implying this pluton is syn-$D_3$. This pluton extends across the north lobe of the Bremner Glacier and is ~20 km in length. Sisson et al. (1989) referred to this pluton as the Bremner Glacier pluton, and determined that it is >50 Ma based on $^{40}Ar/^{39}Ar$ dating of amphibole and is associated with a few other small plutons that have a similar mesoscopic foliation. Tight to isoclinal $D_3$ folds are only present in this region directly adjacent to tonalite intrusions associated with later phases of deformation, perhaps as a combined result of making room for the magma body, and localization of higher finite strains due to the thermal anomaly associated with the intrusion process. Some of the variation in $L_{ext}$ and $L_{gw}$ orientations throughout the Fan Glacier/Bremner Glacier transects might be explained by the intrusion of the Bremner Glacier pluton. Since the pluton is post-$D_2$ to syn-$D_3$, emplacement of such a large body would have to deform the preexisting $D_2$ structure, including $L_{ext}$ and $L_{gw}$ orientations. However, the emplacement of the late phase Bremner Glacier pluton does not explain the great variations in orientation of $L_{ext}$ and $L_{gw}$ in the areas that are not directly adjacent to the Bremner Glacier pluton. It is most likely that the observed variation in $L_{ext}$ and $L_{gw}$ orientations throughout the Fan Glacier/Bremner Glacier transects is also due to overprinting of the fabrics and lineations associated with $D_2$ during $D_3$ deformation and the associated formation of the dextral shear zone system in the CMC.

### Turtle Rocks Creek Transect

The Turtle Rocks Creek transect has been described previously in some detail by Pavlis and Sisson (2003); however, we revisited this field area to examine structural details associated with the major $D_3$ dextral shear zone recognized in this area (Fig. 2). The geologic map and stereonet plots of fabric and structural orientation data for the Turtle Rocks Creek transect is presented in Plate 3. The same metamorphic rock units are present in the Turtle Rocks Creek map area as in the Fan Glacier/Bremner Glaciers map areas, but their structural attitude is different. Specifically, this region represents a clear exposure of a down-plunge view of the structures that form the CMC, as the metamorphic isograds, and the schist-gneiss transition, turn from an overall E-W strike along the northern edge of the CMC into N-S strikes with gentle west dips. As a result of the change in macroscopic structural orientation, the Turtle Rocks Creek map area offers a unique down-plunge exposure of the $D_3$ Bremner shear zone at the schist to gneiss transition (Plate 5-7).

The Bremner shear zone, as described by Pavlis and Sisson (2003), is a vertical, northwest-trending zone of $D_3$ dextral shear at the western termination of Transition Glacier. Rapid melting has caused Transition Glacier to recede in recent years, allowing new portions of the Bremner shear zone to be observed and mapped since the time of Pavlis and Sisson's (2003) field work. In this paper, we have divided the map area into two domains: Domain $1^{TR}$ for the region adjacent to the southern side of the Bremner shear zone, and Domain $2^{TR}$ for the area within the Bremner shear zone (Plate 5-7).

Rocks in Domain $1^{TR}$ are predominantly transitional gneiss; however, the top of the transitional gneiss zone is also exposed with amphibolite grade schist directly adjacent to the Bremner shear zone included in this domain. In the transitional gneiss south of Transition Glacier, $D_2$ folds are reclined, subisoclinal to isoclinal, gentle to moderately plunging folds ($F_{2AP}$ $L_{F2}$) with a continuous axial planar cleavage ($S_2$). $S_2$ foliations in both the transitional gneiss and structurally overlying schist have shallow to moderate northwest dips, and associated $L_{ext}$ are gently to moderately northwest plunging. $D_3$ structures deform older $S_2$ foliations into

upright, open to close, gentle to moderately west-plunging folds ($F_{3AP}$, $L_{F3}$). $D_3$ also deforms older $S_2$ and $F_{2AP}$, forming type 3 fold interference patterns.

Cordierite σ clasts with top-to-the-east shear sense are observed in the transition gneiss (Fig. 4C). Cordierite asymmetries are also supported by quartz *c*-axis fabrics from deformed quartz veins within this area, which show similar top east shear sense (Day, 2007). These observations indicate $D_2$ top-to-the-east shear along a subhorizontal plane, parallel to the transitional gneiss layering, as well as parallel to the $S_2$ fabrics. Steeply dipping dextral shear bands, however, are also present and indicate an approximately vertical plane of shear superimposed on $D_2$ fabrics at a high angle to layering in the transitional gneiss as well as the macroscopic mapped trace of the transitional gneiss. Since both the shear bands and $D_3$ folds deform older $D_2$ fabrics, they almost certainly formed at the same time, during $D_3$.

Domain $2^{TR}$ covers rocks within the Bremner shear zone (Plate 5-7; Fig. 2). Our new mapping in Domain $2^{TR}$ is mostly within amphibolite grade schist directly above the transitional gneiss. There is a sharp contrast in deformation style and apparent finite strain between the schist within Domain $1^{TR}$ and the schist within the Bremner shear zone in Domain $2^{TR}$. $D_1$ structures in Domain $2^{TR}$ are observed as a gentle to moderately northeast-southwest–dipping foliation ($S_1$). However, $S_1$ is deformed by $D_2$ structures, which in Domain $2^{TR}$ are reclined, gentle to moderately northwest plunging isoclinal folds ($F_{2AP}$, $L_{F2}$) with an axial planar continuous cleavage ($S_2$). $L_{ext}$ measured parallel to $S_2$ foliations are moderately northwest plunging. $S_{gw}$ and $L_{gw}$, which form a finite strain fabric and lineation, have orientations similar to $S_2$ and $L_{ext}$. $D_3$ structures within the shear zone are upright, close to tight, gentle to moderately plunging folds ($F_{3AP}$, $L_{F3}$) with a steeply dipping crenulation cleavage. $D_3$ folds in the Bremner shear zone have a tighter interlimb angle than those in Domain $1^{TR}$, and range in size from macroscopic folds (~1–2 km) to outcrop scale to crenulations deforming individual biotite layers.

C′ shear bands are observed throughout Domain $2^{TR}$, and have a steep northeast dip (Fig. 4D). Shear bands are similar to those in the transitional gneiss in Domain $1^{TR}$, except that shear bands are more pervasive in the Bremner shear zone. These shear bands are $D_3$ structures, as they cut and deform $S_2$, and have a dextral shear sense. $F_3$ fold axes ($L_{F3}$) form an oblique angle with these shear bands, and deform syn-$D_2$ tonalite intrusions into asymmetric boudins (Fig. 4E), which are both indicative of wrenching motion during $D_3$ dextral motion within the Bremner shear zone.

Tonalite intrusions are also observed within the Bremner shear zone (Plates 3 and 5-7). A prominent pluton on the northern side of the map area contains biotite, solid-state foliations that are approximately parallel to $S_2$ in the surrounding schist, indicating that it formed as a syn-$D_2$ intrusion. $S_2$ foliations within this body indicate that this pluton is folded into an open, $D_3$ synform, probably during dextral shearing in the shear zone. Small fingers of syn-$D_2$ tonalite are also deformed into asymmetric boudin chains by $D_3$ dextral shear bands. These are similar to structures previously described by Pavlis and Sisson (2003; Figs. 4D and 4E).

### Wernicke Glacier Transect

A $D_3$ dextral shear zone had been previously recognized within the schist at the western termination of the CMC between the Wernicke and Van Cleve glaciers (Pavlis and Sisson, 2003; Fig. 2). The geologic map and stereonet plots of fabric and structural orientation data for the Wernicke Glacier transect is presented in Plate 4. We reexamined this locality to extend that mapping and examine the down-plunge geometry of the $D_3$ dextral shear zone. This area is also important in that a series of plutons were emplaced within this shear zone, along the gneiss transition. Thus, in addition to the down-plunge view of another $D_3$ shear zone, the Wernicke Glacier map area also offers a view of the effects of extensive plutonism on the transition gneiss.

$D_2$ fabric in the Wernicke Glacier map area varies in orientation from shallowly to moderately, southwest to northwest dipping. This $D_2$ fabric is an axial planar continuous cleavage ($S_2$), however, only a few $D_2$ folds were observed in this area. $S_{gw}$, the finite strain fabric, observed at Wernicke Glacier is oriented similar to $S_2$, except it is dominantly west dipping. Extensional lineations—$L_{gw}$ and $L_{ext}$—observed on $S_{gw}$ and $S_2$ foliation planes, respectively, are shallowly to moderately, northwest plunging. $D_3$ structures are observed to deform $S_2$ into upright, moderately northwest-plunging folds ($F_{3AP}$, $L_{F3}$; Fig. 4F). The few $D_2$ folds observed are also deformed into type 3 interference pattern folds. As in the other parts of the western CMC, $D_3$ fold interlimb angles vary from close to tight in the gneiss and close to open in the overlying amphibolite grade schist and transition gneiss. However, close to tight $D_3$ folds are observed in the transition gneiss within the Wernicke Glacier shear zone.

Shear sense indicators, such as σ and δ clasts, C′ shear bands, and asymmetric quartz vein boudins, are common in the transitional gneiss zone, and display a top to the east shear sense. This top-to-the-east shear sense is parallel to the transition gneiss contacts. Of the few subvertically oriented C′ shear bands observed in the Wernicke Glacier shear zone, most exhibit a dextral shear sense; however, some do exhibit a sinistral shear sense. The presence of these shear bands and tight $D_3$ folds suggests that a wrenching mechanism of deformation occurred in the Wernicke Glacier shear zone, similar to that observed in the Bremner shear zone and Harry's Gulch shear zone.

A significant variation in the thickness of the transition gneiss unit is observed within the Wernicke Glacier map area. Variation in the thickness of the transitional gneiss corresponds to regions outside of and within the Wernicke Glacier shear zone. In the regions adjacent to the Wernicke Glacier shear zone, thickness of the transition gneiss zone is ~400 m, similar to that observed by Pavlis and Sisson (2003) in several other locations in the CMC (Plate 5-8). However, the thickness of the transition gneiss increases dramatically to ~1.5 km within the boundaries of the Wernicke Glacier shear zone. An important feature of this area, however, is that the thickness of the transitional gneiss unit is directly correlated to the abundance of multiple generations of tonalitic plutons. Based on cross-cutting relationships with generations of foliations, this plutonic suite varies from syn-$D_2$, pre- to syn-$D_3$, or post-$D_3$, however, the syn-$D_3$ plutons have the largest exposed areas. The overlap of the Wernicke Glacier shear zone and the increase in transition gneiss thickness suggest that thickening of the transition gneiss is a result of horizontal shortening during $D_3$ dextral shearing, potentially aided by thermal effects of the large, syn-$D_3$ plutonic injections.

### Western CMC Structure Summary

On the north and south sides of the Bremner River canyon, $S_2$ foliation comprises two distinct, mappable flat belts (Plate 1). Domain $1^{HG}$ and Fan Glacier/Bremner Glacier (Plate 2) are also similar in structural characteristics and can be included with the northern flat-belt region. Domain $1^{TR}$ (Plate 3) has similar structural characteristics and can be included in the southern flat-belt region. Domains in the Bremner River canyon located between the two flat-belt regions that have steeply dipping $S_2$ foliation are grouped into a central steep belt (Plate 1). Due to the steeply oriented fabrics, higher finite strain, and abundance of $D_3$ folds and shear bands, we interpret this central region as a $D_3$ Bremner River shear zone (Plate 1). Domain $2^{TR}$ (Plate 3) is also part of the Bremner shear

zone, and Domain $2^{HR}$ (Plate 2) and Wernicke Glacier (Plate 4) also represent separate, yet similar, steeply oriented dextral shear zones that formed as part of the $D_3$ CMC strike-slip system (Fig. 5).

## DISCUSSION

### Structure of the Bremner River Valley: Cleavage Fan or Macroscopic Folding?

With completion of our mapping in the Fan Glacier and Bremner Glacier area, it now seems clear that the apparent cleavage fan initially described by O'Driscoll (2006) and Day (2007) is in fact an oversimplified structural interpretation for the CMC. Instead, it is apparent that the steepening of $S_2$ foliation toward the Bremner River in the western transects is a geometric coincidence of two large-scale $D_3$ folds with the valley walls, giving rise to an apparent cleavage fan when, in fact, the poorly exposed rocks of the Bremner valley simply represent a train of upright $D_3$ folds formed in a transcurrent tectonic environment. We have shown in this paper that $S_2$ in the amphibolite grade schist and transition gneiss appears to have formed extensive $D_2$ flat belts, before being refolded during $D_3$. However, from our observations of relative ages of the structures, no $D_2$ strike-slip shear zones are recognized in the western CMC, only $D_3$ strike-slip shear zones. $D_3$ deforms the $D_2$ flat belts into conspicuous, large-scale, open folds in the amphibolite grade schist and transitional gneiss adjacent to the $D_3$ dextral shear zones, and into tight, conspicuous folds; these zones are interpreted as $D_3$ shear zones. $F_{3AP}$ orientations, which are analogous to a $D_3$ cleavage, are steep throughout the western CMC (>60°), and are not observed to steepen or shallow in dip moving toward or away from $D_3$ shear zones.

In the attachment zone models, vertical strike-slip shear zones are represented by a symmetrical convergence of steep fabrics during shearing, forming a cleavage fan. However, in the western CMC, deformation in the shear zones is preserved as conspicuous $D_3$ folds that can be viewed as either large antiforms or synforms. Individual $D_3$ structures are not continuous and parallel to the entire length of the $D_3$ shear zones, as might be predicted by attachment zone models. Rather, $D_3$ folds have axes that are oblique to the shear zone boundaries, due to $D_3$ wrenching motion. In regions of the western CMC adjacent to $D_3$ dextral shear zones $D_3$ folds form either symmetric or asymmetric geometries. The Harry's Gulch shear zone, Bremner shear zone, and the Wernicke Glacier shear zone (Plate 5-8) exhibit asymmetric $D_3$ fold geometries with a synformal structure on one side, and an antiformal structure on the opposing side of the $D_3$ shear zones. This deformation pattern is similar to the fault-fold relationships observed in compression tectonic regimes, where an anticline forms in the hanging wall of a thrust fault, and a syncline will form in the footwall. In other locations of the Bremner shear zone, a symmetric $D_3$ fold geometry is observed, with antiforms adjacent to both sides of the $D_3$ shear zone boundary (Plate 5-8). However, despite the symmetric appearance in some areas, this is part of the overall asymmetry in cleavage patterns adjacent to the $D_3$ shear zones.

Looking at the regional characteristics of the structural geometry, a map scale pattern emerges that can be related to the style and pattern of $D_3$ deformation observed at smaller scales within the $D_3$ shear zones. Wrench folding associated with dextral shear bands is the dominant form of deformation during $D_3$ within the shear zones. Since $D_3$ folds exist outside the localized high finite strain of the multiple shear zones described in the region, wrench folding on a larger scale is likely to be the mechanism of deformation forming these structures. The $D_3$ dextral shear zones are basically dextral shear bands that exist at a macroscopic scale. This wrenching motion would have also generated horizontal shortening and thickening of the transition gneiss during $D_3$ dextral shearing. This was potentially aided by thermal effects of large syn-$D_3$ plutonic injections, as observed in the Wernicke Glacier shear zone. Continuing dextral shear along the lengths of the $D_3$ shear zones creates wrenching motion in the areas between the shear zones. In the same way that mesoscopic structures vary within shear zones, this wrenching motion deforms the foliations of the $D_2$ flat belts into the observed $D_3$ folds, between the shear zones. However, the open $D_3$ folds overprint the $D_2$ flat belts formed at lower finite strains than the tighter $D_3$ folds in the shear zones, behaving as semirigid blocks in between the shear zones.

It is evident from our work and previous work (Pavlis and Sisson, 1995, 2003) as well as recent work by Gasser (2010) that $D_3$ in the CMC represents a dextral transpression strike-slip system superimposed on earlier $D_1$ and $D_2$ fabrics (Fig. 6). Moreover, this $D_3$ shear overlaps in time with a period of dextral strike-slip reactivation on the Border Ranges fault (Roeske et al., 2003; Pavlis and Roeske, 2007). This temporal overlap implies that the entire high-temperature ductile deformation history of the CMC is closely tied to strike-slip along the tectonic backstop to the complex, the Border Ranges fault. This raises important questions on the general tectonic setting of the $D_2$-$D_3$ progressive deformation within the CMC, as it suggests both phases are linked to a strike-slip dominated system developed during plate motion changes associated with ridge subduction.

### Characteristics of the Brittle to Ductile Transition in Strike-Slip Systems

One of the most complete exposures of a dextral shear zone in the CMC strike-slip system is the combined Stuart Creek fault and Harry's Gulch shear zone (Plates 1 and 2, Fig. 5). Exposures of the brittle Stuart Creek fault can be traced through many of the Bremner River valley transects, and is along strike with the ductile Harry's Gulch shear zone (Fig. 5, Plates 5-4 and 5-5). Since the western CMC can be treated as a down plunge view the combined Stuart Creek and Harry's Gulch shear zone is an excellent exposure to observe the characteristics of the transition from brittle to ductile deformation in strike-slip systems, and its associated structure. Brittle deformation within the Stuart Creek fault is constrained to a discrete zone, ~20 m in width where the fault is well exposed. However, across the brittle-ductile transition, the width of the ductile deformation zone increases in the Harry's Gulch shear zone to ~2.5 km, but is still constrained to a localized zone of high finite strain within the greenschist grade schists.

This relationship suggests that where the brittle shear zone reaches the ductile transition, the discrete slip on the fault passes downward into a narrow zone characterized by tight, upright $D_3$ folds representing wrench folds superimposed on the earlier, nearly flat-lying $D_2$ fabric. This observation indicates that displacement along the shear bands created $D_3$ folds by wrenching motion within the shear zones, which is consistent with a wrench tectonics setting initially described by the studies of Wilcox et al. (1973).

Evidence from the larger Bremner shear zone also shows that the dextral shear zones in the ductile domain have an anastomosing map pattern similar to the pattern commonly shown by brittle faults in the near surface environment. This anastomosing shear zone pattern is best seen by the inclusion of large, weakly deformed, lenses of amphibolite grade schist completely within the Bremner shear zone (Fig. 5).

It is not yet understood how the discrete shear along the brittle fault is transferred downward into a 2-km-wide shear zone in part because of incomplete exposure. Nonetheless, based on limited observations near the structurally lowest known level of the Stewart Creek fault and the highest known structural level of the Harry's Gulch shear zone, it appears that $S_3$ fabrics probably converge upward, toward the brittle fault. This is a relationship predicted by many theoretical models (e.g., Teyssier and Cruz, 2004).

Overall, these characteristics suggest that at these crustal levels, strike-slip faults remain in a localized vertical zone of deformation even after passing well into the ductile domain; however, as seen elsewhere, the localized zone of deformation becomes wider in the ductile domain relative to the brittle domain.

### Deep Crustal Structure of Transpressional Systems

From the discussion above, it is observed that in this region, strike-slip shear zones maintain steep dips as they pass far into the ductile deformation domain of the crust as originally presented by Scholz (1990, p. 129). However, these observations of strike-slip shear zones in the CMC raise questions about the overall structure in the deep crust as deformation passes into rocks near, or at, their melting temperatures in the gneissic rocks. Specifically, we evaluate two hypotheses for the deep crustal structure in this transpressional system: (1) the existence of a narrow detachment zone at the schist-gneiss boundary, and (2) masking of the vertical, high-strain shear zones in the gneiss core created by thinner layering in the metamorphic fabric.

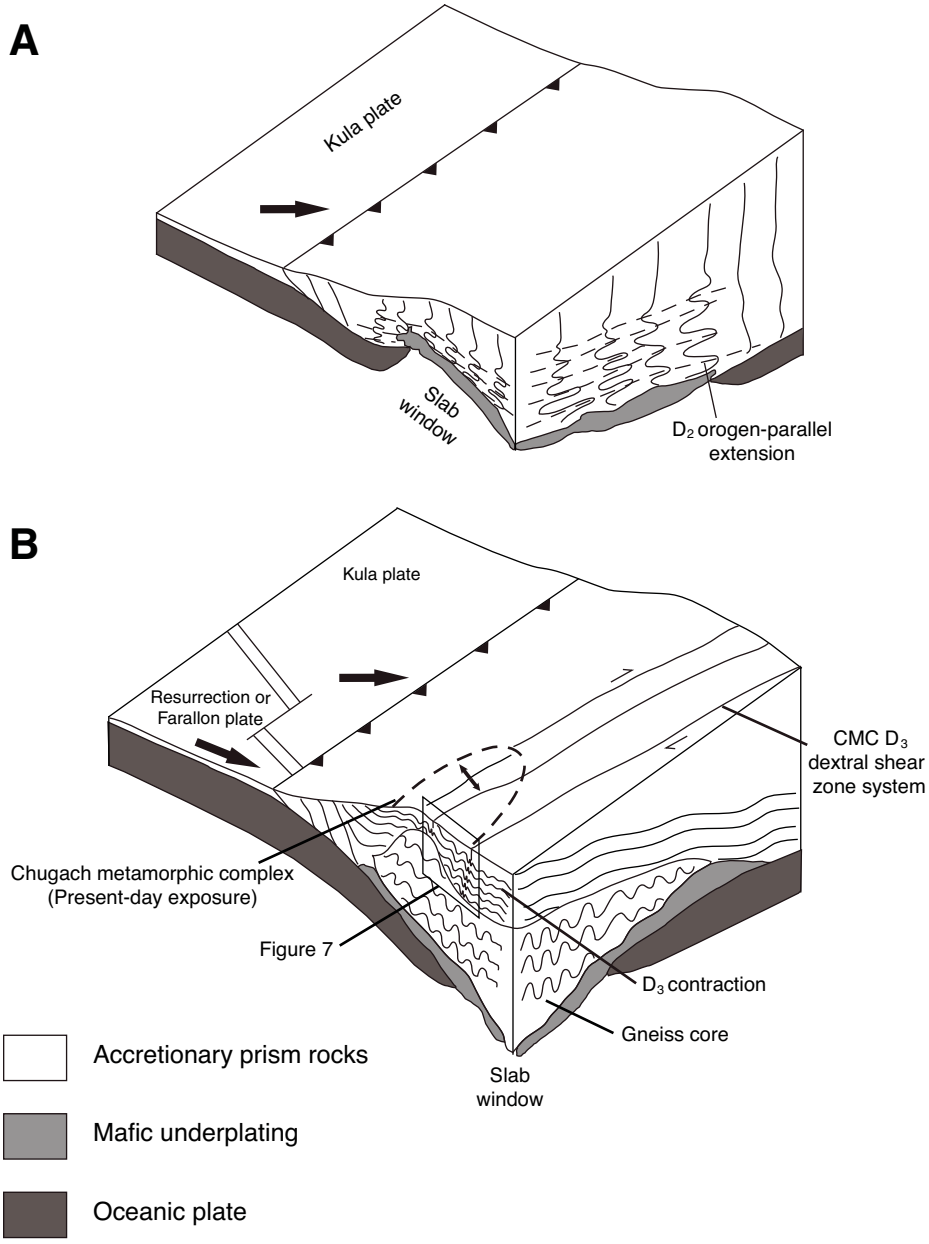


**Figure 6. Summary of the progressive deformation sequence during formation of the CMC. (A) $D_2$ deformation, which progressively forms the shallowly dipping $S_2$ foliation, and roughly orogen parallel extensional lineations. (B) $D_3$ deformation, which forms the dextral transpression system and associated shear zones in the schist layers of the CMC. Transpression creates wrench folds both within the vertical shear zones and in the more rigid blocks between shear zones, as well as throughout the gneiss core. This wrenching motion is also responsible for the resulting antiformal shape of the gneiss core. The box indicates the location of Figure 7. Figure modified from Sisson and Pavlis (1993).**

In addition to the difference in deformation style between the shear zones and the adjacent regions in the schist layers, another difference in deformational style exists between the schist envelope and the gneiss core of the CMC. From the descriptions above it is clear that there is a widespread distinction in structural style between the schist to the transition gneiss versus the structurally underlying gneiss core. In the schists, $D_3$ fold structures are characterized by open interlimb angles and are typically large-scale, long-wavelength, map-scale features as shown in the cross sections (Plates 5-3 –5-6). $D_3$ folds differ greatly, however, in the gneiss core. Folds are smaller scale, with wavelengths down to cm scale, typically show tight interlimb angles, and deep within the gneiss core descriptions by Gasser (2010) indicate $D_3$ structures completely transpose $S_2$. Collectively these observations suggest that $D_3$ finite strains are distinctly higher within the gneiss, similar to the higher finite strains observed within the $D_3$ shear zones, but the strain is more homogeneously distributed. Based on work by Gasser (2010), it appears that higher strains are recorded deep within the gneissic core, yet mapping is insufficient to determine if this relationship represents convergence of anastomosing shear zones (e.g., Bremner and Wernicke Glacier shear zones) into a single shear zone, or some more complex flow pattern. Nonetheless, as first noted by Pavlis and Sisson (2003), the distinction in structural style between the gneiss and schist is striking and suggests very different mechanical behavior during deformation. Specifically, these differences in finite strains, fold characteristics, and shear localization suggest a spatial difference in the vertical crustal column of deformation and strain during the $D_3$ phase of deformation, and this distinction has important implications for the behavior of strike-slip systems as they penetrate into zones of extensive partial melting, or near melting conditions represented by the gneiss.

We suggest that the vertical difference in structural style within the CMC crustal column could be explained by two distinct mechanisms (Fig. 7). The first hypothesis (Fig. 7A) is analogous to the interpretations of Pavlis and Sisson

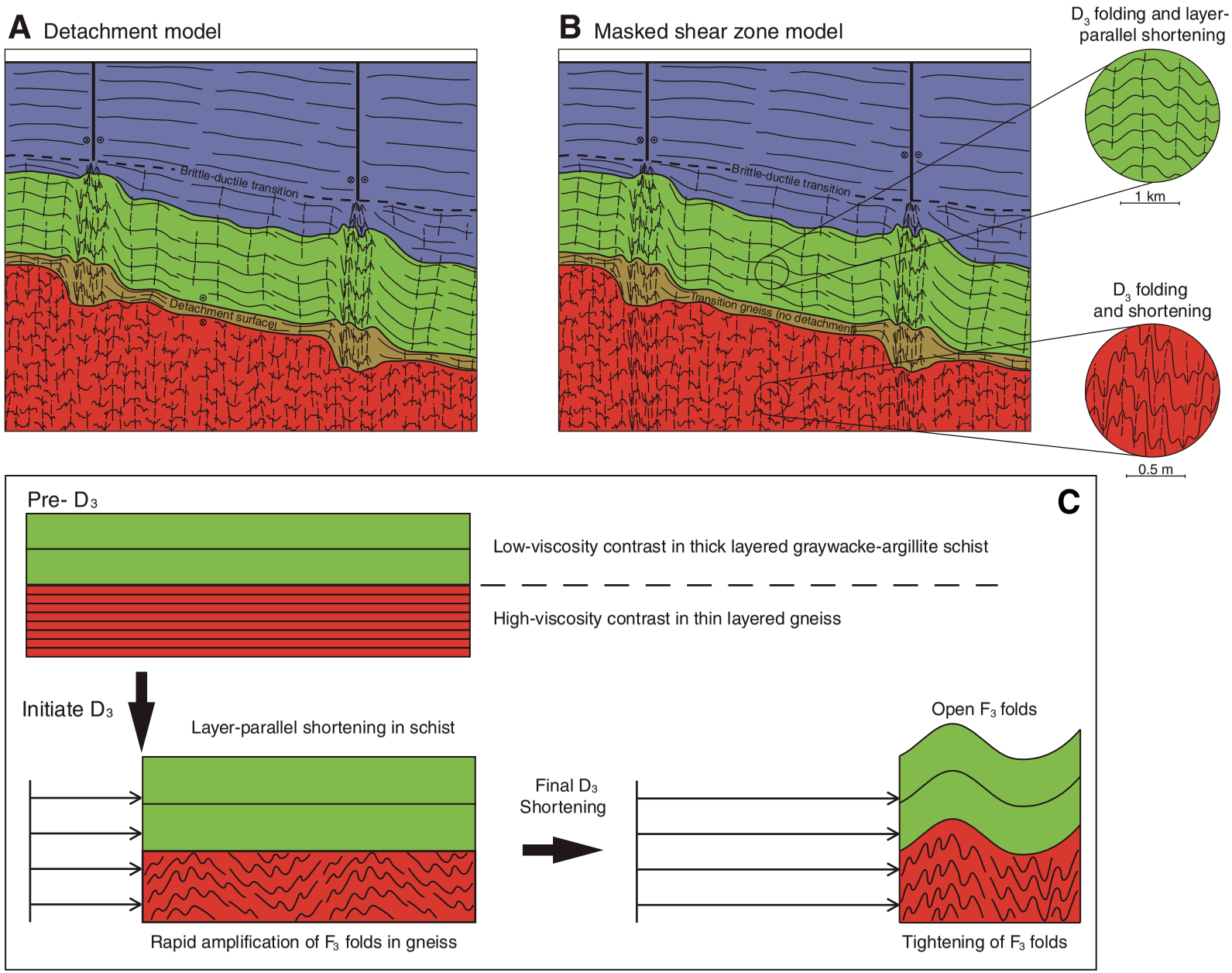


**Figure 7. Proposed alternative models for the deep structure of strike-slip systems indicated by the $D_3$ deformation of the CMC. (A) Simple detachment model with detachment between lower crustal flow and middle crustal shear zones at the gneiss transition. (B) Masked shear zone model where variations in fold style with different structural levels are attributed to wavelength selection and variable degrees of layer-parallel shortening during $D_3$. (C) Schematic illustration of the $D_3$ progressive deformational sequence for the masked shear zone model. See text for detailed discussion.**

(2003) and suggests the presence of a $D_3$ crustal detachment surface along the gneiss transition. In this hypothesis, the sharp change in distribution of strain and style of $D_3$ deformation over a narrow zone implies the existence of a detachment surface and would indirectly imply that $D_3$ reused $D_2$ fabrics along this horizon during development of the detachment. In this model, the continuous cleavage along the gneiss transition is a composite $D_2$-$D_3$ fabric, developed by subhorizontal shear between upper crustal blocks bounded by shear zones (Bremner, Wernicke, and Harry's Gulch shear zones) and distributed deformation in the gneiss. This hypothesis is supported weakly by shear sense indicators within and near the gneiss transition that shows reversals across the Bremner shear zone (top-to-the-east in the south, top-to-the-west in the north). Nonetheless, these relationships could be coincidental, and in either case are difficult to reconcile with clear steeply dipping $D_3$ fabric superpositions within the transitional gneiss.

An alternative hypothesis (Fig. 7B) for variations in structural style with depth in the CMC is that there is no detachment, and the distinctions in style are the product of fold wavelength selection effects in a heterogeneous material. In this hypothesis, the principal explanation for the variation in structural style between the gneiss and schist are the observed differences in metasedimentary layer thickness, variations in layer viscosity contrast, or both. It has long been known that layer thickness is directly proportional to fold wavelength of rocks deformed in the ductile domain (e.g., Smith, 1975, 1977). Qualitatively, this theory is obvious in that thicker layers will always produce longer wavelength folds under equivalent conditions. In the context of the CMC, thinly laminated, segregated mafic and felsic bands, in addition to layers of partial melt in the gneiss, represent very thin layers (1 cm or less) that would naturally develop into short-wavelength, mesoscopic folds. In contrast, original sedimentary layering is still well preserved in the schists, and throughout the schist there are large bands of massive graywacke, commonly more than 100 m thick. If the dominant layers in these schists are 100 m thick or more, the folds should also be comparably larger or macroscopic scale structures. Indeed, in the western termination of the CMC, there are large-scale $D_3$ folds with wavelengths of 2–3 km (e.g., Pavlis and Sisson, 2003).

An important feature of this hypothesis is that shorter-wavelength folds in the migmatitic gneiss would lead to the appearance of homogeneously distributed $D_3$ strains in the gneiss core versus localized shear within the overlying transition gneiss and schist layers, when in reality both are folded, but at different wavelengths and different amplitudes due to variable fold amplification (Fig. 7B). This type of strain partitioning is attractive theoretically, but would initially require variable components of $D_3$ layer parallel shortening in the schists relative to the gneiss to accommodate the general variations in fold style (Fig. 7C). Variable layer parallel shortening is predicted by fold theory where fold amplification rates are directly related to layer viscosity contrast (Ramberg, 1964). In our case (Figs. 7A and 7B), outside of $D_3$ shear zones, the $D_3$ folds have large interlimb angles (typically >100°) in the schist and have wavelengths on the order of kilometers. Throughout the gneiss interlimb angles are lower (typically <60°) and have wavelengths on the order of cm to meters. This distinction in interlimb angle and fold wavelength seemingly implies large differences in $D_3$ strain. However, if layer viscosity contrast was markedly lower in the schist than the gneiss, the total $D_3$ shortening could be comparable between the schist and gneiss, but fold amplitudes would be lower in schist, masking the $D_3$ shortening as cryptic layer-parallel shortening (Fig. 7).

We suggest that at present these hypotheses are not resolvable. We suspect the second hypothesis (Figs. 7B and 7C) is more likely, but could only be tested through detailed analysis of $D_3$ folds at different structural levels and additional detailed mapping into gneiss to determine if discrete shear zones can be traced through the gneiss core or the deformation truly dissipates over a larger volume of rock.

## CONCLUSION

The final phase of deformation in the CMC ($D_3$) records formation of a dextral strike-slip system superimposed on earlier deformational periods, and the unusual down-plunge view provides constraints on deformation at different crustal levels in a strike-slip system. Our observations suggest that the attachment zone model of Teyssier and Cruz (2004), and the cleavage fan pattern predicted by the model, are not applicable to this region as previously thought. Instead, anastomosing shear zones penetrate the crustal section through amphibolite facies schists. Wrench folds are prevalent, both within dextral shear zones, as well as in the more rigid blocks of schist between the shear zones. Instead of a symmetric cleavage fan, an asymmetric cleavage pattern is recognized in the CMC, and is concurrent with wrenching motion throughout the region associated with the last phase of deformation ($D_3$) during formation of the CMC.

Unique exposure of different levels in the CMC strike-slip system provides important constraints on general structural characteristics of strike-slip faults as they pass from the brittle to the ductile domain. Across the brittle-ductile transition, a discrete strike-slip fault passes downward into a narrow, ~2-km-wide, localized zone of high finite strain. At deeper structural levels, these distinct dextral shear zones can be traced structurally downward to the core of the CMC where they disappear into a broad region of migmatitic gneiss. However, it is not yet clear how deformation is dispersed within the gneiss and we suggest two alternative hypotheses that are not easily distinguished. Although we reject the hypothesis of an attachment zone transferring subhorizontal shear between dextral shear zones, detachment along a subhorizontal shear zone remains an allowable hypothesis. Alternatively, the sharp change in the style of $D_3$ folds across the gneiss transition from smaller wavelength folds with tight interlimb angles in the gneiss to large wavelength folds with open interlimb angles in the overlying transition gneiss and schist may be entirely the result of a wavelength selection process with short wavelength folds in thinly laminated gneiss versus larger-scale folds with a significant component of layer-parallel shortening in the schists.

### ACKNOWLEDGMENTS

Scharman conducted this work in partial fulfillment of the requirements for the degree of Ph.D. in Geology at the University of Texas at El Paso. This work was supported by NSF grants EAR-0711105 and EAR-0229939 awarded to Pavlis, and a GSA Graduate Student grant awarded to Scharman. We thank Kurt Stüwe, Deta Gasser, and Emilie Bruand at Karl Franzens University of Graz for insightful discussions and sharing field logistics. Jasper Konter provided an insightful, informal review. We appreciate Roberto Cruz, Hugo Rodriguez, Chris Carson, and Matt Cannon for their field assistance. We are also grateful to Paul Claus for helping us with travel logistics in this region.

### REFERENCES CITED

Amato, J.M., and Pavlis, T.L., 2010, Detrital zircon ages from the Chugach terrane, southern Alaska, reveal multiple episodes of accretion and erosion in a subduction complex: Geology, v. 38, p. 459–462, doi: 10.1130/G30719.1.

Bradley, D., Kusky, T., Haeussler, P., Goldfarb, R., Miller, M., Dumoulin, J., Nelson, S.W., and Karl, S., 2003, Geologic signature of early Tertiary ridge subduction in Alaska, *in* Sisson, V.B., Roeske, S.M., and Pavlis, T.L., eds., Geology of a transpressional orogen developed during ridge-trench interaction along the North Pacific margin: Boulder, Colorado, Geological Society of America Special Paper 371, p. 19–49.

Day, E., 2007, Characterization of structures and deformation in the brittle-ductile transition, western termination of the Chugach metamorphic complex, southern Alaska [Master's thesis]: University of New Orleans, 57 p.

Dewey, J.F., Holdsworth, R.E., and Strachan, R.A., 1998, Transpression and transtension zones, *in* Holdsworth, R.E., Strachan, R.A., and Dewey, J.F., eds.,

Continental Transpressional and Transtensional Tectonics: London, Geological Society Special Publications 135, p. 1–14.

Dewey, J.F., 2002, Transtension in arcs and orogens: International Geology Review, v. 44, p. 402–439, doi: 10.2747/0020-6814.44.5.402.

Dusel-Bacon, C., 1994, Metamorphic history in Alaska, *in* Plafker, G., and Berg, H.C., eds., The geology of Alaska: Boulder, Colorado, Geological Society of America, Geology of North America, v. G-1, p. 389–450.

Fitch, T.J., 1972, Plate Convergence, Transcurrent Faults, and Internal Deformation Adjacent to Southeast Asia and the Western Pacific: Journal of Geophysical Research, v. 77, p. 4432–4460, doi: 10.1029/JB077i023p04432.

Gasser, D., 2010, Evolution of the Chugach Metamorphic Complex in southern Alaska in space and time [Ph.D. thesis]: Karl Franzens University of Graz Austria, 315 p.

Gasser, D., Bruand, E., Stüwe, K., Foster, D.A., Schuster, R., Fügenschuh, B., and Pavlis, T., 2011, Formation of a metamorphic complex along an obliquely convergent margin: Structural and thermochronological evolution of the Chugach Metamorphic Complex, southern Alaska: Tectonics, v. 30, doi:10.1029/2010TC002776.

Haeussler, P.J., Bradley, D., Goldfarb, R., Snee, L., and Taylor, C., 1995, Link between ridge subduction and gold mineralization in southern Alaska: Geology, v. 23, p. 995–998, doi: 10.1130/0091-7613(1995)023<0995:LBRSAG>2.3.CO;2.

Hudson, T., 1979, Mesozoic plutonic belts of southern Alaska: Geology, v. 7, p. 230–234, doi: 10.1130/0091-7613(1979)7<230:MPBOSA>2.0.CO;2.

Hudson, T., and Plafker, G., 1982, Paleogene metamorphism of an accretionary flysch terrane, eastern Gulf of Alaska: Geological Society of America Bulletin, v. 93, p. 1280–1290, doi: 10.1130/0016-7606(1982)93<1280:PMOAAF>2.0.CO;2.

Hudson, T., Plafker, G., and Peterman, Z.E., 1979, Paleogene anatexis along the Gulf of Alaska margin: Geology, v. 7, p. 573–577, doi: 10.1130/0091-7613(1979)7<573:PAATGO>2.0.CO;2.

Karig, D.E., 1980, Material transport within accretionary prisms and the "knocker" problem: The Journal of Geology, v. 88, p. 27–39, doi: 10.1086/628471.

Marshak, R.S., and Karig, D.E., 1977, Triple junctions as a cause for anomalously near-trench igneous activity between the trench and volcanic arc: Geology, v. 5, p. 233–236, doi: 10.1130/0091-7613(1977)5<233:TJAACF>2.0.CO;2.

Nokleberg, W.J., Plafker, G., Lull, J.S., Wallace, W.K., and Winkler, G.R., 1989, Structural analysis of the Southern Peninsular, Southern Wrangellia, and Northern Chugach Terranes along the Trans-Alaska Crustal Transect, Northern Chugach Mountains, Alaska: Journal of Geophysical Research, v. 94, p. 4297–4320, doi: 10.1029/JB094iB04p04297.

O'Driscoll, L.J., Pavlis, T.L., and Day, E., 2005, Complex crustal stratification in a ductile attachment zone within the Chugach metamorphic complex, southern Alaska: Geological Society of America Abstracts with Programs, v. 37, p. 552.

O'Driscoll, L., 2006, Complex crustal stratification within the Chugach Mountains, southern Alaska [Master's thesis]: New Orleans, Louisiana, University of New Orleans, 52 p.

Pavlis, T.L., Day, E., and O'Driscoll, L.J., 2006, Evolution of a mid-crustal strike-slip system during prograde metamorphism: The Chugach metamorphic complex, eastern Chugach Mountains, Alaska: Geological Society of America Abstracts with Programs, v. 38, p. 78.

Pavlis, T.L., and Roeske, S.M., 2007, The Border Ranges fault system, southern Alaska, *in* Ridgway, K.D., Trop, J.M., Glen, J.M.G., and O'Neill, J.M., eds., Tectonic growth of a collisional Continental Margin: Crustal evolution of Southern Alaska: Geological Society of America Special Paper 431, p. 95–128.

Pavlis, T.L., and Sisson, V.B., 1995, Structural history of the Chugach metamorphic complex in the Tana River region, eastern Alaska: A record of Eocene ridge subduction: Geological Society of America Bulletin, v. 107, no. 11, p. 1333–1355, doi: 10.1130/0016-7606(1995)107<1333:SHOTCM>2.3.CO;2.

Pavlis, T. L., and Sisson, V.B., 2003, Development of a subhorizontal decoupling horizon in a transpressional system, Chugach metamorphic complex, Alaska: Evidence for rheological stratification of the crust, *in* Sisson, V.B., Roeske, S.M., and Pavlis, T.L., eds., Geology of a transpressional orogen developed during ridge-trench interaction along the North Pacific margin: Boulder, Colorado, Geological Society of America Special Paper 371, p. 191–216.

Pavlis, T.L., Marty, K., and Sisson, V.B., 2003, Constrictional flow within the Eocene forearc of Southern Alaska; an effect of dextral shear during ridge subduction, *in* Sisson, V.B., Roeske, S.M., and Pavlis, T.L., eds., Geology of a transpressional orogen developed during ridge-trench interaction along the North Pacific margin: Boulder, Colorado, Geological Society of America Special Paper 371, p. 171–190.

Pavlis, T.L., Langford, R., Hurtado, J., and Serpa, L., 2010, Computer-based data acquisition and visualization systems in field geology: Results from 12 years of experimentation and future potential: Geosphere, v. 6, no. 3, p. 275–294.

Plafker, G., Moore, J.C., and Winker, G.R., 1994, Geology of the southern Alaska margin, *in* Plafker, G., and Berg, H.C., eds., The geology of Alaska: Boulder, Colorado, Geological Society of America, Geology of North America, v. G-1, p. 389–450.

Plafker, G., Nokleberg, W.J., and Lull, J.S., 1989, Bedrock geology and tectonic evolution of the Wrangellia, Penninsular, and Chugach terranes along the Trans-Alaska crustal transect in the Chugach Mountains and southern Copper River Basin, Alaska: Journal of Geophysical Research, v. 94, no. B4, p. 4255–4295, doi: 10.1029/JB094iB04p04255.

Ramberg, H., 1964, Selective buckling of composite layers with contrasted rheological properties: A theory for simultaneous formation of several orders of folds: Tectonophysics, v. 1, p. 307–341, doi: 10.1016/0040-1951(64)90020-4.

Richter, D.H., Preller, C.C., Labay, K.A., and Shew, N.B., 2005, Geology of Wrangell-Saint Elias National Park and Preserve, south-central Alaska: U.S. Geological Survey Scientific Investigations Series Map SIM-2877, scale 1:350,000.

Roeske, S.M., Snee, L.W., and Pavlis, T.L., 2003, Dextral-slip reactivation of an arc-forearc boundary during Late Cretaceous-early Eocene oblique convergence in the northern Cordillera, *in* Sisson, V.B., Roeske, S.M., and Pavlis, T.L., eds., Geology of a transpressional orogen developed during ridge-trench interaction along the North Pacific margin: Boulder, Colorado, Geological Society of America Special Paper 371, p. 171–190.

Scholz, C.H., 1990, The Mechanics of earthquakes and faulting: Cambridge, Cambridge University Press, p. 129.

Serpa, L., and Pavlis, T.L., 1996, Three-dimensional model of the late Cenozoic history of the Death Valley region, southeastern California: Tectonics, v. 15, p. 1113–1128, doi: 10.1029/96TC01633.

Sisson, V.B., and Pavlis, T.L., 1993, Geological consequences of plate reorganization: An example from the Eocene southern Alaska fore arc: Geology, v. 21, no. 10, p. 913–916, doi: 10.1130/0091-7613(1993)021<0913:GCOPRA>2.3.CO;2.

Sisson, V.B., Hollister, L.S., and Onstott, T.C., 1989, Petrologic and age constraints on the origin of a low-pressure/high-temperature metamorphic complex, southern Alaska: Journal of Geophysical Research, v. 94, p. 4392–4410, doi: 10.1029/JB094iB04p04392.

Smith, R.B., 1975, Unified theory of the onset of folding, boudinage, and mullion structure: Geological Society of America Bulletin, v. 86, p. 1601–1609, doi: 10.1130/0016-7606(1975)86<1601:UTOTOO>2.0.CO;2.

Smith, R.B., 1977, Formation of folds, boudinage, and mullions in non-Newtonian materials: Geological Society of America Bulletin, v. 88, p. 312–320, doi: 10.1130/0016-7606(1977)88<312:FOFBAM>2.0.CO;2.

Teyssier, C., and Cruz, L., 2004, Strain gradients in transpressional to transtensional attachment zones, *in* Grocott, J., McCaffrey, K.J.W., Taylor, G., and Tikoff, B., eds., Vertical coupling and decoupling in the lithosphere: London, Geological Society Special Publications 227, p. 101–115.

Thatcher, W., 1995, Microplate versus continuum descriptions of active tectonic deformation: Journal of Geophysical Research, v. 100, no. B3, p. 3885–3894, doi: 10.1029/94JB03064.

Wilcox, R.E., Harding, T.P., and Seely, D.R., 1973, Basic wrench tectonics: American Association of Petroleum Geologists, v. 57, no. 1, p. 74–96.

Manuscript Received 29 September 2010
Revised Manuscript Received 27 January 2011
Manuscript Accepted 3 February 2011